SUPPLEMENTARY INFORMATION

Metallic Radionuclide-labeled Tetrameric 2,6-Diisopropylphenyl Azides for Cancer Treatment

Yudai Ode,[a] Ambara R. Pradipta,*[a] Akihiro Ishiwata,[b] Akihiro Nambu,[c] Kazunobu Ohnuki,[d] Hiroshi Mizuma,[e,f] Hiromitsu Haba [c] and Katsunori Tanaka *[a,b]

[a] *Department of Chemical Science and Engineering, School of Materials and Chemical Technology, Tokyo Institute of Technology, 2-12-1 Ookayama, Meguro, Tokyo 152-8552, Japan.*

[b] *Biofunctional Synthetic Chemistry Laboratory, RIKEN Cluster for Pioneering Research, 2-1 Hirosawa, Wako, Saitama 351-0198, Japan.*

[c] *Nuclear Chemistry Group, RIKEN Nishina Center for Accelerator-Based Science, 2-1 Hirosawa, Wako, Saitama 351-0198, Japan.*

[d] *Exploratory Oncology Research and Clinical Trial Center, National Cancer Center, 6-5-1 Kashiwanoha, Kashiwa, Chiba 277-8577, Japan.*

[e] *Department of Functional Brain Imaging, National Institutes for Quantum Science and Technology (QST), 4-9-1 Anagawa, Inage-ku, Chiba-shi, Chiba 263-8555, Japan.*

[f] *Laboratory for Pathophysiological and Health Science, RIKEN Center for Biosystems Dynamics Research, Minatojima-minamimachi, Chuo-ku, Kobe, Hyogo 650-0047, Japan*

* *Corresponding author emails:*
pradipta.a.aa@m.titech.ac.jp (Ambara R. Pradipta)
tanaka.k.dg@m.titech.ac.jp (Katsunori Tanaka)

Keywords: acrolein; aryl azide; [3+2] cycloaddition; in vivo synthesis; radiometal

Table of Contents

Previous study

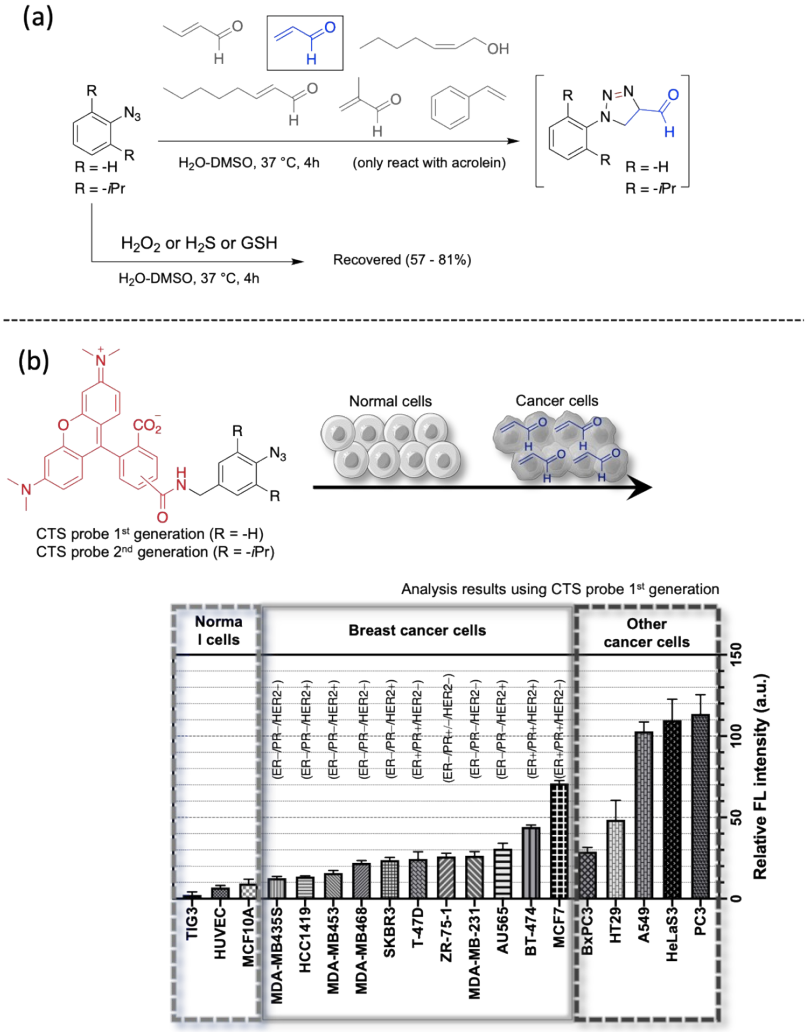

Fig. S1 Our previous work: (a) Phenyl azide reacts selectively towards acrolein under physiological conditions. No noticeable products were found when it was reacted with other α,β-unsaturated aldehydes (*e.g.*, methacrolein, crotonaldehyde, *trans*-2-octenal) or reactive olefin (*e.g.*, cis-2-heptanol, styrene). We found that phenyl azide is stable toward the *in vivo* oxidating and reducing agents, such as H_2O_2, H_2S, and GSH. (b) Acrolein levels in various human cells were determined using a CTS probe. The fluorescence intensity corresponds to the level of acrolein in cells.

Chemical synthesis

All commercially available reagents were used without further purification. The $^{111}InCl_3$ solution was produced by Nihon Medi-Physics Co., Ltd. The $^{90}YCl_3$ solution was obtained from Eckert & Ziegler Radiopharma GmbH. Both $[^{111}In]Cl_3$ and $[^{90}Y]Cl_3$ solutions were dried and diluted with hydrochloric acid to the appropriate concentration before being used in the experiments. The preparative separation was performed by column chromatography on Merck Silica gel 60 (230–400 mesh). High-resolution mass spectrometry (HRMS) was recorded on micrOTOF-QIII. ^1H and ^{13}C NMR spectra were recorded on the Bruker Ascend 400 NMR spectrometer. Unless otherwise mentioned, $CDCl_3$ was used as a solvent, and chemical shifts were represented as δ-values relative to the internal standard TMS.

Caution: Azide-containing compounds are presumed to be potentially explosive. Although we have never experienced such an explosion with the azide compounds used in this study, all manipulations should be carefully carried out in a hood.

Synthesis of bis(4-azido-3,5-diisopropylbenzyl)amine **9**

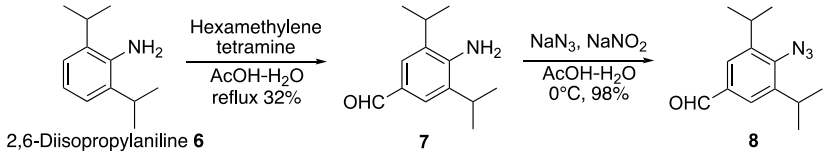

2,6-Diisopropylaniline **6** **7** **8**

*Synthesis of 4-amino-3,5-diisopropylbenzaldehyde **7**:* Hexamethylenetetramine (8.5 g, 61 mmol, 2.0 eq) was added to a solution of 2,6-diisopropylaniline **6** (5.3 g, 30 mmol, 1.0 eq) in AcOH and H_2O (3:1) (100 mL, [2,6-diisopropylaniline **6**] = 0.30 M). The mixture was refluxed with stirring for 30 minutes, cooled to ambient temperature, and evaporated. 20 wt% KOHaq was added until the suspension achieved a pH of 8. The mixture was extracted with EtOAc. The combined organic layer was washed with brine, dried over Na_2SO_4, and filtered. The filtrate was concentrated to dryness under reduced pressure. The residue was purified by Yamazen smart flash column chromatography on silica gel using a gradient of eluents [*n*-hexane/EtOAc (85:15 to 67:33)] to give the desired 4-amino-3,5-diisopropylbenzaldehyde **7** as a white solid (1.9 g, 32% yield). ^1H NMR (400 MHz, $CDCl_3$) δ 9.78 (s, 1H), 7.58 (s, 2H), 4.36 (s, 2H), 2.88 (hept, *J* = 6.7 Hz, 2H), 1.31 (d, *J* = 6.8 Hz, 12H); ^{13}C NMR (101 MHz, $CDCl_3$) δ 191.6, 146.9, 131.7, 127.4, 125.9, 28.0, 22.3; ESI-HRMS m/z calcd for $C_{13}H_{19}NNaO$ ($[M+Na]^+$) 228.1359, found 228.1359.

*Synthesis of 4-azido-3,5-diisopropylbenzaldehyde **8**:* sodium azide (750 mg, 12 mmol, 2.4 eq) was slowly added to a mixture of compound **7** (980 mg, 4.8 mmol, 1.0 eq) and Sodium nitrite (790 mg, 12 mmol, 2.5 eq) dissolved in AcOH and H_2O (5:1) (48 mL, [**7**] = 0.10 M) at 0 °C. After stirring for 1 hour at 0 °C, a saturated aqueous solution of $NaHCO_3$ was added until the mixture achieved a pH of 7. The mixture was extracted with EtOAc. The combined organic layer was washed with brine, dried over Na_2SO_4, and filtered. The filtrate was concentrated to dryness under reduced pressure. The residue was purified by Yamazen smart flash column chromatography on silica gel using a gradient of eluents [*n*-hexane/EtOAc (100:0 to 95:5)] to give the desired 4-azido-3,5-diisopropylbenzaldehyde **8** as a colorless oil (1.1 g, 98% yield). ^{1}H NMR (400 MHz, $CDCl_3$) δ 9.96 (s, 1H), 7.66 (s, 2H), 3.40 (hept, *J* = 6.8 Hz, 2H), 1.31 (d, *J* = 6.8 Hz, 12H); ^{13}C NMR (101 MHz, $CDCl_3$) δ 191.9, 144.2, 140.9, 134.6, 125.8, 28.9, 23.5.; ESI-HRMS m/z calcd for $C_{14}H_{21}N_3NaO_2$ ([M+MeOH+Na]$^+$) 286.1526, found 286.1524.

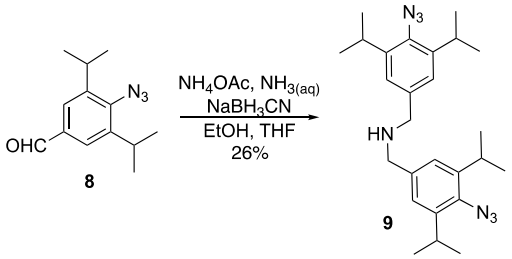

*Synthesis of bis(4-azido-3,5-diisopropylbenzyl)amine **9**:* Compound **8** (500 mg, 2.1 mmol, 1.0 eq) was dissolved in saturated solution of NH_4OAc in EtOH 16 mL, 28% aqueous NH_3 5.6 mL, AcOH 14 mL and THF 3 mL. $NaBH_3CN$ was dissolved in a saturated solution of NH_4OAc in EtOH 5 mL. Compound **8** solution was added dropwise to the $NaBH_3CN$ solution over 7 min ([**8**] = 0.050 M). After stirring for 5 hours at ambient temperature, a saturated aqueous solution of $NaHCO_3$ was added until the mixture achieved a pH of 8. The mixture was extracted with EtOAc. The combined organic layer was washed with brine, dried over Na_2SO_4, and filtered. The filtrate was concentrated to dryness under reduced pressure. The residue was purified by Yamazen smart flash column chromatography on silica gel using eluent [*n*-hexane/EtOAc (9:1)] to give the desired bis(4-azido-3,5-diisopropylbenzyl)amine **9** as a yellow solid (120 mg, 26% yield). ^{1}H NMR (400 MHz, $CDCl_3$) δ 7.11 (s, 4H), 3.77 (s, 4H), 3.35 (hept, *J* = 6.9 Hz, 4H), 1.27 (d, *J* = 6.8 Hz, 24H); ^{13}C NMR (101 MHz, $CDCl_3$) δ 143.3, 138.9, 134.2, 123.8, 53.2, 29.0, 23.7.; ESI-HRMS m/z calcd for $C_{26}H_{38}N_7$ ([M+H]$^+$) 448.3183, found 448.3183.

Synthesis of bis(3,5-diisopropylbenzyl)amine **S7**

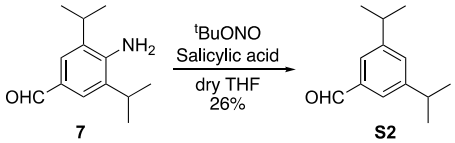

*Synthesis of 3,5-diisopropylbenzaldehyde **S2*** [1]: ^{t}BuONO (980 μL, 8.4 mmol, 1.5 eq) and salicylic acid (100 mg, 0.73 mmol, 0.13 eq) were added to compound **7** (1.4 g, 5.8 mmol, 1.0 eq) in dry THF (24 mL, [**7**] = 0.24 M). The reaction mixture was stirred under an argon atmosphere at ambient temperature for 3 hours. The resulting mixture was extracted with EtOAc. The combined organic layer was washed with brine, dried over Na_2SO_4, and filtered. The filtrate was concentrated to dryness under reduced pressure. The residue was purified by Yamazen smart flash column chromatography on silica gel using n-hexane as eluent to give the desired 3,5-diisopropyl benzaldehyde **S2** as a yellow oil (280 mg, 26% yield). ^{1}H NMR (400 MHz, $CDCl_3$) δ 9.99 (s, 1H), 7.57 (d, *J* = 1.7 Hz, 2H), 7.35 (t, *J* = 1.8 Hz, 1H), 2.98 (hept, *J* = 6.9 Hz, 2H), 1.29 (d, *J* = 6.9 Hz, 12H); ^{13}C NMR (101 MHz, $CDCl_3$) δ 193.1, 150.0, 136.9, 131.7, 125.5, 34.2, 24.0; ESI-HRMS m/z calcd for $C_{14}H_{22}NaO_2$ ($[M+MeOH+Na]^+$) 245.1512, found 245.1509.

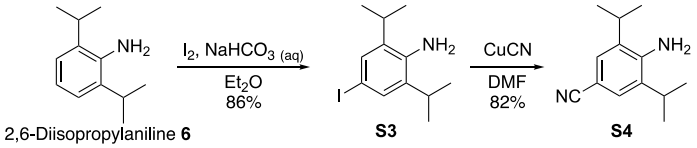

*Synthesis of 4-iodo-2,6-diisopropylaniline **S3*** [2]: According to the literature, 4-iodo-2,6-diisopropylaniline **S3** was obtained as a red-black oil (9.3 g, 86% yield). ^{1}H NMR (400 MHz, $CDCl_3$, 25 °C) δ 7.27 (s, 2H), 3.73 (bs, 2H, NH_2), 2.84 (hept, *J* = 6.7 Hz, 2H), 1.24 (d, *J* = 6.8 Hz, 12H); ^{13}C NMR (100 MHz, $CDCl_3$, 25 °C) δ 140.2, 135.2, 131.9, 81.3, 28.0, 22.4.; ESI-HRMS m/z calcd for $C_{12}H_{19}IN$ ($[M+H]^+$) 304.0557, found 304.0558.

*Synthesis of 4-amino-3,5-diisopropylbenzonitrile **S4*** [2]: According to the literature, 4-amino-3,5-diisopropylbenzonitrile **S4** was obtained as a yellow solid (3.0 g, 82% yield). ^{1}H NMR (400 MHz, $CDCl_3$, 25 °C) δ 7.29 (s, 2H), 4.21 (s, 2H, NH_2), 2.85 (hept, *J* = 6.7 Hz, 2H), 1.27 (d, *J* = 6.8 Hz, 12H); ^{13}C NMR (100 MHz, $CDCl_3$) δ 144.9, 132.3, 127.5, 121.3, 100.3, 27.8, 22.0.; ESI-HRMS m/z calcd for $C_{13}H_{18}N_2Na$ ($[M+Na]^+$) 225.1362, found 225.1362.

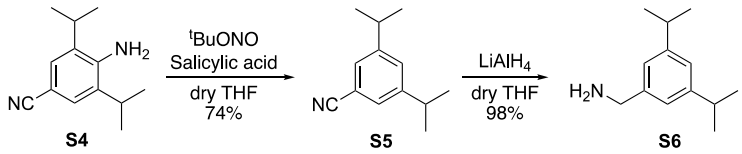

S4 **S5** **S6**

*Synthesis of 3,5-diisopropylbenzonitrile **S5*** [1]: ^{t}BuONO (741 μL, 6.4 mmol, 1.2 eq) and salicylic acid (760 mg, 5.5 mmol, 1.0 eq) were added to compound **S4** (1.1 g, 5.3 mmol, 1.0 eq) in dry THF (18 mL, [**S4**] = 0.30 M). The reaction mixture was stirred under an argon atmosphere at ambient temperature for 5.5 hours. The resulting mixture was extracted with EtOAc. The combined organic layer was washed with brine, dried over Na_2SO_4, and filtered. The filtrate was concentrated to dryness under reduced pressure. The residue was purified by Yamazen smart flash column chromatography on silica gel using a gradient of eluents [*n*-hexane/EtOAc (100:0 to 97:3)] to give the desired 3,5-diisopropyl benzonitrile **S5** as a colorless oil (740 mg, 74% yield). ^{1}H NMR (400 MHz, $CDCl_3$) δ 7.33 (d, *J* = 1.7 Hz, 2H), 7.29 (t, *J* = 1.6 Hz, 1H), 2.91 (hept, *J* = 6.9 Hz, 2H), 1.25 (d, *J* = 6.9 Hz, 12H); ^{13}C NMR (101 MHz, $CDCl_3$) δ 150.2, 129.9, 127.7, 119.7, 112.3, 34.1, 23.9.; ESI-HRMS m/z calcd for $C_{13}H_{17}NNa$ ($[M+Na]^+$) 210.1253, found 210.1257.

*Synthesis of (3,5-diisopropylphenyl)methanamine **S6***: $LiAlH_4$ (360 mg, 9.4 mmol, 6.2 eq) was slowly added to a solution of 3,5-diisopropylbenzonitrile **S5** (280 mg, 1.5 mmol, 1.0 eq) in dry THF 15 mL ([**S5**] = 0.30 M) at 0 °C. After stirring the reaction mixture under an argon atmosphere at ambient temperature for 3 hours, a saturated aqueous solution of Rochelle salt was added dropwise to the reaction mixture at 0 °C. EtOAc was then added and stirred for 30 minutes. The mixture was extracted with EtOAc. The combined organic layer was washed with brine, dried over Na_2SO_4, and filtered. The filtrate was concentrated to dryness under reduced pressure. The residue was purified by Yamazen smart flash column chromatography on silica gel using a gradient of eluents [*n*-hexane/EtOAc (90:10 to 84:16)] to give the desired (3,5-diisopropylphenyl) methanamine **S6** as a yellow oil (280 mg, 98% yield). ^{1}H NMR (400 MHz, $CDCl_3$) δ 7.00 (d, *J* = 1.7 Hz, 2H), 6.97 (t, *J* = 1.8 Hz, 1H), 3.84 (s, 2H), 2.89 (hept, *J* = 6.9 Hz, 2H), 1.26 (d, *J* = 6.9 Hz, 12H); ^{13}C NMR (101 MHz, $CDCl_3$) δ 149.4, 143.3, 123.4, 122.8, 46.9, 34.4, 24.2.; ESI-HRMS m/z calcd for $C_{13}H_{21}NNa$ ($[M+Na]^+$) 214.1566, found 214.1566.

References: (1) D. Felipe-Blanco, F. Alonso and J. C. Gonzalez-Gomez, *Adv. Synth. Catal.*, 2017, **359**, 2857-2863; (2) A. R. Pradipta, H. Michiba, A. Kubo, M. Fujii, T. Tanei, K. Morimoto, K. Shimazu and K. Tanaka, *Bull. Chem. Soc. Jpn.*, 2022, **95**, 421-426.

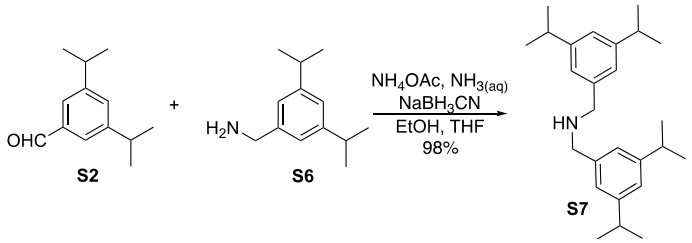

*Synthesis of bis(3,5-diisopropylbenzyl)amine **S7**:* Compound **S6** (180 mg, 0.92 mmol, 1.3 eq), AcOH 410 µL, and $NaBH_3(CN)$ (90 mg, 1.4 mmol, 2.1 eq) were added to compound **S2** (130 mg, 0.69 mmol, 1.0 eq) in EtOH (6.9 mL, [**S2**] = 0.10 M). After stirring for 22 hours at ambient temperature, the reaction mixture was evaporated and extracted with EtOAc. The combined organic layer was washed with brine, dried over Na_2SO_4, and filtered. The filtrate was concentrated to dryness under reduced pressure. The residue was purified by Yamazen smart flash column chromatography on silica gel using eluent [*n*-hexane/EtOAc (4:1)] to give the desired bis(3,5-diisopropyl benzyl)amine **S7** as a colorless oil (250 mg, 98% yield). ^{1}H NMR (400 MHz, $CDCl_3$) δ 7.03 (d, *J* = 1.7 Hz, 4H), 6.98 (t, *J* = 1.7 Hz, 2H), 3.80 (s, 4H), 2.89 (hept, *J* = 6.9 Hz, 4H), 1.25 (d, *J* = 6.9 Hz, 24H); ^{13}C NMR (101 MHz, $CDCl_3$) δ 149.1, 140.4, 123.8, 123.5, 53.7, 34.3, 24.2.; ESI-HRMS m/z calcd for $C_{26}H_{40}N$ ($[M+H]^+$) 366.3155, found 366.3154.

Synthesis of DOTA-2PhN$_3$ **10**

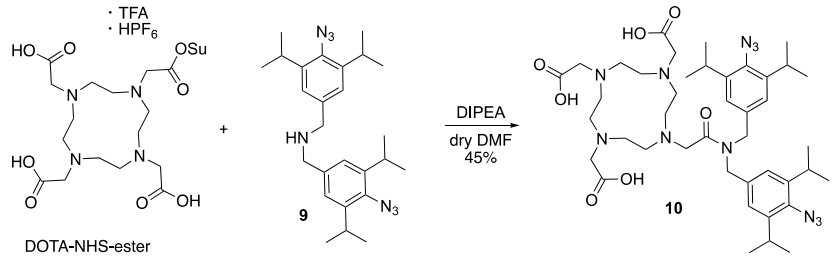

*Synthesis of 2,2',2''-(10-(2-(bis(4-azido-3,5-diisopropylbenzyl)amino)-2-oxoethyl)-1,4,7,10-tetraazacyclododecane-1,4,7-triyl)triacetic acid **10** (DOTA-2PhN$_3$ **10**)*: DOTA-NHS-ester(170 mg, 0.23 mmol, 2.0 eq) and DIPEA (120 µL, 0.69 mmol, 6.0 eq) were added to compound **9** (51 mg, 0.11 mmol, 1.0 eq) in dry DMF (1.2 mL, [**9**] = 0.10 M). The reaction mixture was stirred under an argon atmosphere at ambient temperature for 20 hours. The mixture was purified by reversed-phase (RP)-HPLC (mobile phase A, 0.1% TFA in H_2O; B, 0.1% TFA in CH_3CN) to give the DOTA-2PhN$_3$ **10** (in TFA salt form) as a white solid (49 mg, 45%). Conditions of RP-HPLC(Shimadzu): Column, Cosmosil 5C$_{18}$-AR-300 (Nacalai Tesque, Inc.) 20 × 250 mm; Gradient elution, 0 – 3 min at 50% B, 3 – 14 min at 50 – 100% B, 14 – 18 min at 100% B; Flow rate: 10 mL/min (Pump LC-20AP); UV detection at 254 nm (UV/vis detector SPD-20AV).

The desired DOTA-2PhN$_3$ **10** was eluted at 14 minutes. ^{1}H NMR (400 MHz, CD_3CN) δ 6.98 (s, 2H), 6.77 (s, 2H), 4.51 (s, 4H), 4.04 (s, 2H), 3.93 (s, 2H), 3.75 (s, 2H), 3.65 (s, 2H), 3.43 – 2.97 (m, 20H), 1.13 (dd, *J* = 9.0, 6.9 Hz, 24H); ^{13}C NMR (101 MHz, CD_3CN) δ 161.0, 160.7, 160.3, 160.0, 144.4, 144.2, 136.5, 135.6, 135.1, 125.8, 123.9, 121.4, 118.5, 115.6, 112.7, 54.3, 51.8, 49.7, 29.7, 29.7, 23.7, 23.7; ESI-HRMS m/z calcd for $C_{42}H_{64}N_{11}O_7$ ($[M+H]^+$) 834.4985, found 834.4987.

Synthesis of DOTA-2PhH **S8**

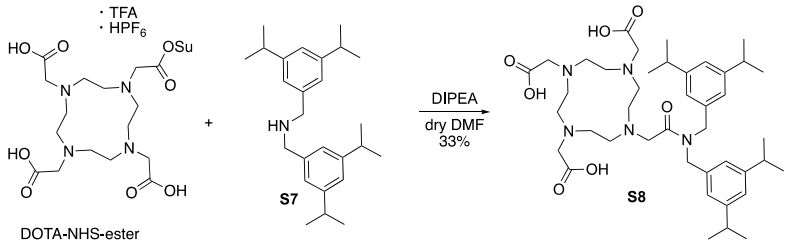

*Synthesis of 2,2',2''-(10-(2-(bis(3,5-diisopropylbenzyl)amino)-2-oxoethyl)-1,4,7,10-tetra-azacyclododecane-1,4,7-triyl)triacetic acid **S8** (DOTA-2PhH **S8**)*: DOTA-NHS-ester(98 mg, 0.13 mmol, 1.5 eq) and DIPEA (86 µL, 0.50 mmol, 6.0 eq) were added to compound **S7** (31 mg, 0.084 mmol, 1.0 eq) in dry DMF (0.85 mL, [**S7**] = 0.10 M). The reaction mixture was stirred under an argon atmosphere at ambient temperature for 3.5 days. The mixture was purified by reversed-phase (RP)-HPLC (mobile phase A, 0.1% TFA in H_2O; B, 0.1% TFA in CH_3CN) to give the DOTA-2PhH **S8** (in TFA salt form) as a white solid (24 mg, 33%). Conditions of RP-HPLC(Shimadzu): Column, Cosmosil $5C_{18}$-AR-300 (Nacalai Tesque, Inc.) 20 × 250 mm; Gradient elution, 0 – 3 min at 50% B, 3 – 14 min at 50 – 100% B, 14 – 23 min at 100% B; Flow rate: 10 mL/min (Pump LC-20AP); UV detection at 254 nm (UV/vis detector SPD-20AV).

The desired DOTA-2PhH **S8** was eluted at 13 minutes. ^{1}H NMR (400 MHz, CD_3CN:D_2O = 1:1) δ 7.04 (s, 2H), 6.89 (d, *J* = 1.7 Hz, 2H), 6.76 (d, *J* = 1.7 Hz, 2H), 4.52 (s, 2H), 4.37 (s, 2H), 4.15 (s, 2H), 3.80 (s, 2H), 3.62 (s, 4H), 3.29 (s, 8H), 2.86 – 2.78 (m, 4H), 1.15 (dd, *J* = 6.9, 3.5 Hz, 24H); ^{13}C NMR (101 MHz, CD_3CN) δ 161.5, 161.1, 150.6, 150.3, 143.9, 137.6, 136.6, 125.3, 124.7, 124.6, 123.8, 116.3, 34.8, 24.4; ESI-HRMS m/z calcd for $C_{42}H_{65}N_5NaO_7$ ($[M+Na]^+$) 774.4776, found 774.4771.

Synthesis of DTPA-4PhN$_3$ **11**

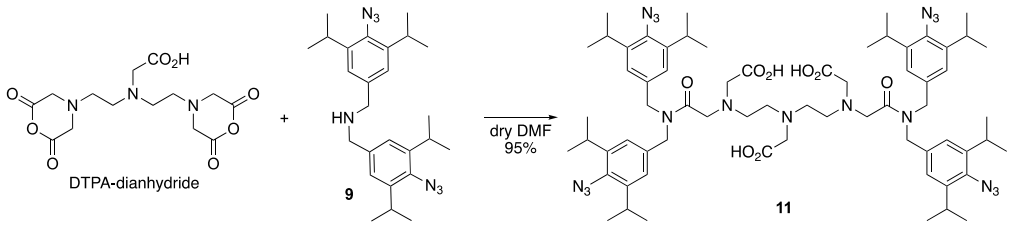

*Synthesis of 2-(4-azido-3,5-diisopropylbenzyl)-1-(4-azido-3,5-diisopropylphenyl)-11-(2-(bis(4-azido-3,5-diisopropylbenzyl)amino)-2-oxoethyl)-5,8-bis(carboxymethyl)-3-oxo-2,5,8,11-tetraazatridecan-13-oic acid **11** (DTPA-4PhN$_3$ **11**)*: DTPA-dianhydride(19 mg, 0.052 mmol, 1.0 eq) was added to compound **9** (55 mg, 0.12 mmol, 2.3 eq) in dry-DMF (0.50 mL, [DTPA-dianhydride] = 0.10 M). The reaction mixture was stirred under an argon atmosphere at ambient temperature for 20 hours. The mixture was purified by reversed-phase (RP)-HPLC (mobile phase A, 0.1% TFA in H_2O; B, 0.1% TFA in CH_3CN) to give the DTPA-4PhN$_3$ **11** (in TFA salt form) as a yellow solid (66 mg, 95%). Conditions of RP-HPLC(Shimadzu): Column, Cosmosil 5C$_{18}$-AR-300 (Nacalai Tesque, Inc.) 20 × 250 mm; Gradient elution, 0 – 5 min at 80% B, 5 – 10 min at 80 – 100% B, 10 – 20 min at 100% B; Flow rate: 10 mL/min (Pump LC-20AP); UV detection at 254 nm (UV/vis detector SPD-20AV).

The desired DTPA-4PhN$_3$ **11** was eluted at 15 minutes. ^{1}H NMR (400 MHz, CD_3CN) δ 6.95 (s, 4H), 6.82 (s, 4H), 4.52 (s, 4H), 4.41 (s, 4H), 4.28 (s, 4H), 4.08 (s, 4H), 3.66 (s, 2H), 3.44 (t, *J* = 5.9 Hz, 4H), 3.29 – 3.21 (m, 8H), 3.15 (t, *J* = 5.9 Hz, 4H), 1.13 (dd, *J* = 6.9, 1.8 Hz, 48H); ^{13}C NMR (101 MHz, CD_3CN) δ 172.1, 168.9, 167.4, 160.6, 160.2, 144.6, 144.2, 136.1, 135.7, 135.6, 134.8, 125.4, 124.1, 115.5, 58.0, 56.5, 54.6, 54.2, 51.5, 51.4, 50.9, 29.7, 29.6, 23.7, 23.7; ESI-HRMS m/z calcd for $C_{66}H_{94}N_{17}O_8$ ([M+H]$^+$) 1252.7466, found 1252.7462.

Radiolabeling

Procedure A (^{111}In labeling for DOTA compound): 10 μL of 1 M KOAc aqueous solution and 106.5 μL of 4 mM DOTA compound in MeCN were added to 100 μL of [^{111}In]Cl_3 in 5×10^{-2} M HCl aqueous solution. After thorough mixing by pipetting the solution(pH 4), it was heated at 85 °C for 20 minutes and then cooled at room temperature for 5 minutes. In advance, the SPE Cartridge (Waters Sep-Pak tC18 Plus Short Cartridge, WAT036810) was activated with 3 mL of distilled water, and the reaction solution was injected into the cartridge. The syringe was rinsed twice with 50% MeCN distilled water (100 μL each time), and the rinsed solution was injected into the cartridge. After flushing the cartridge with 10 mL of distilled water, 99.5% EtOH (500 μL) was passed through the cartridge four times to elute the ^{111}In-labeled DOTA compound. The radioactivity fraction among the four fractions was collected, heated, and dried at 70 °C. The resulting product was redissolved in an appropriate amount of 10% EtOH saline for animal experiments.

Procedure B (^{111}In labeling for DTPA compound): 100 μL of 0.3 M KOAc aqueous solution and 10 μL of 1 mM DTPA compound in MeCN were added to 100 μL of [^{111}In]Cl_3 in 5×10^{-2} M HCl aqueous solution. After thorough mixing by pipetting the solution, it was left at room temperature for 15 minutes. In advance, the SPE Cartridge (Waters Sep-Pak tC18 Plus Short Cartridge, WAT036810) was activated with 3 mL of distilled water, and the reaction solution was injected into the cartridge. The syringe was rinsed twice with 50% MeCN distilled water (100 μL each time), and the rinsed solution was injected into the cartridge. After flushing the cartridge with 10 mL of distilled water, 99.5% EtOH (500 μL) was passed through the cartridge four times to elute the ^{111}In-labeled DTPA compound. The radioactivity fraction among the four fractions was collected, heated, and dried at 70 °C. The resulting product was redissolved in an appropriate amount of 10% EtOH saline for animal experiments.

Procedure C (^{90}Y labeling for DTPA compound): 100 μL of 0.3 M KOAc aqueous solution and 5 μL of 1 mM DTPA compound in MeCN were added to 10 μL of [^{90}Y]Cl_3 in 5×10^{-2} M HCl aqueous solution. After thorough mixing by pipetting the solution, it was left at room temperature for 15 minutes. In advance, the SPE Cartridge(waters Sep-Pak tC18 Plus Short Cartridge, WAT036810) was activated with 3 mL of distilled water, and the reaction solution was injected into the cartridge. The syringe was rinsed twice with 50% MeCN distilled water (100 μL each time), and the rinsed solution was injected into the cartridge. After flushing the cartridge with 10 mL of distilled water, 99.5% EtOH (500 μL) was passed through the cartridge four times to elute the ^{90}Y-labeled DTPA compound. The radioactivity fraction among the four fractions was collected, heated, and dried at 70 °C. The resulting product was redissolved in an appropriate amount of 10% EtOH saline for animal experiments.

Radio-thin layer chromatography (Radio-TLC) is a technique that separates radiolabeled compounds for analytical work. It is often used to analyze radiolabeled compounds' purity and determine reaction conversion when optimizing radiosynthesis processes. A radio-TLC scanner is used to examine a TLC plate (spotted with a small amount of the sample and then developed with a mobile phase), which moves a radiation detector along the plate to obtain measurements of generated radiation as a function of distance. See Figs. S2-S4.

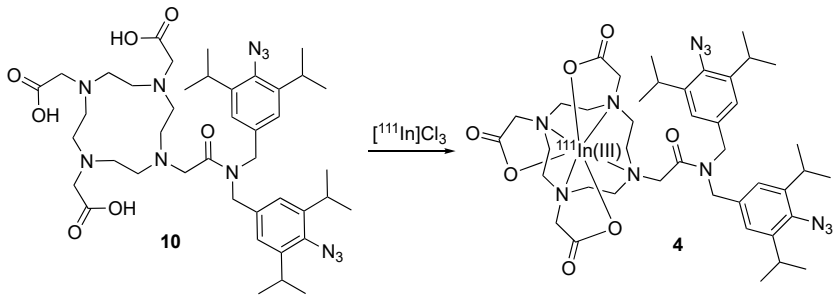

Synthesis of ^{111}In-DOTA-2PhN$_3$ ***4***: This reaction was carried out following Procedure A. Upon reaction and purification with 66.9 MBq of ^{111}In, 56.8 MBq of ^{111}In-DOTA-2PhN$_3$ **4** was obtained. Radiochemical yield (RCY) = 85% (Uncorrected for half-life). Radiochemical purity (RCP) = 100% (100%, after 28 h).

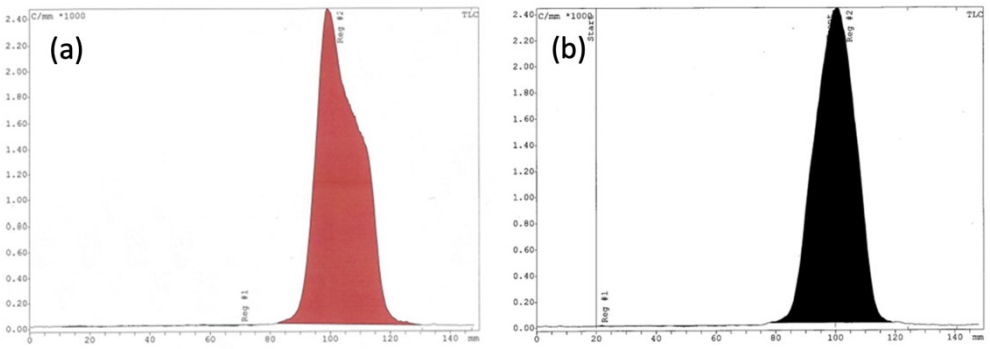

Fig. S2 Radio-TLC chromatogram of the purified compound **4** obtained with the radio-TLC scanner. The horizontal axis represents the distance (mm) along the TLC plate between the observed peak (at 100 mm) and the original start line (at 20 mm) before elution. The vertical axis represents the intensity of radioactivity (counts/minutes). (a) Measurement immediately after purification (RCP 100%). (b) Measurement at 28 hours after purification (RCP 100%). TLC eluent: MeCN/H_2O (1:1).

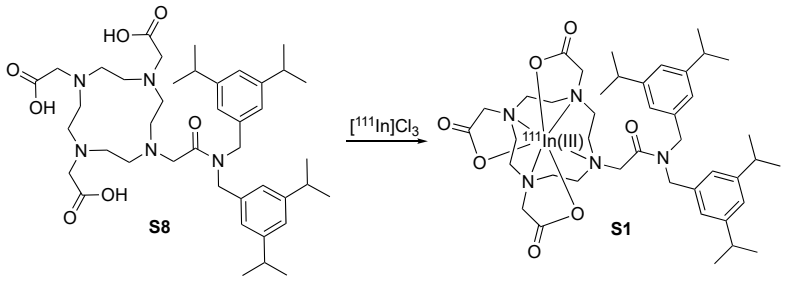

*Synthesis of ^{111}In-DOTA-2PhH **S1***: This reaction was carried out following Procedure A. Upon reaction and purification with 172 MBq of ^{111}In, 160 MBq of ^{111}In-DOTA-2PhH **S1** was obtained. RCY = 93% (Uncorrected for half-life). RCP = 100% (97%, after 24 h).

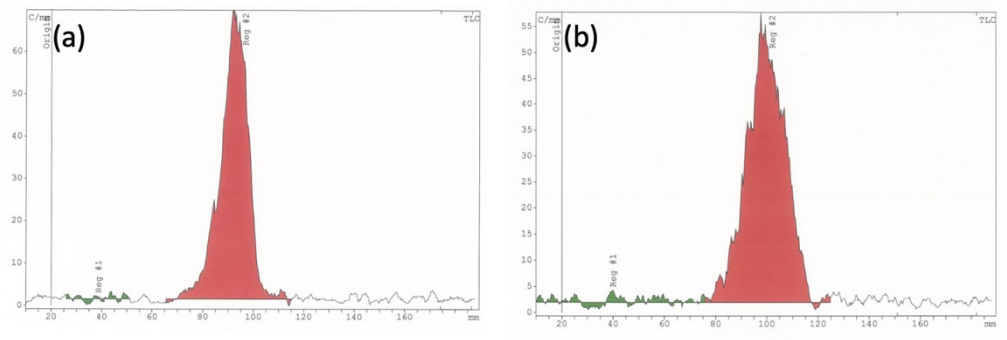

Fig. S3 Radio-TLC chromatogram of the purified compound **S1** obtained with the radio-TLC scanner. The horizontal axis represents the distance (mm) along the TLC plate between the observed peak (at 90 mm) and the original start line (at 20 mm) before elution. The vertical axis represents the intensity of radioactivity (counts/minutes). (a) Measurement immediately after purification (RCP 100%). (b) Measurement at 24 hours after purification (RCP 97%). TLC eluent: MeCN/H_2O (1:1).

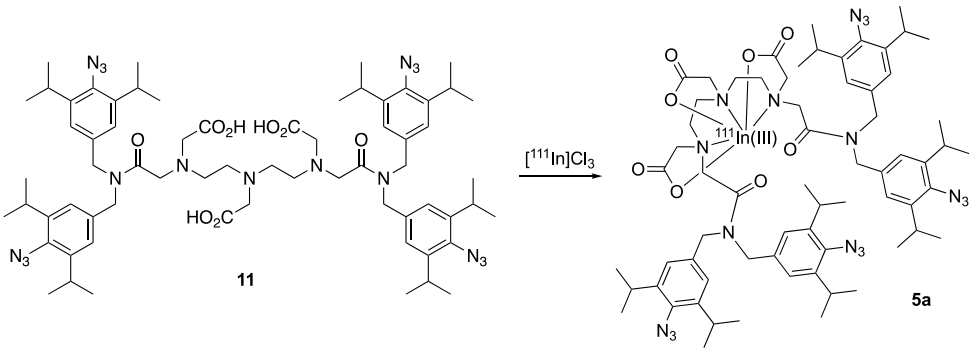

Synthesis of ^{111}*In-DTPA-4PhN*$_3$ ***5a***: This reaction followed Procedure B. Upon reacting and purifying with 170 MBq of ^{111}In, 127 MBq of ^{111}In-DTPA-4PhN$_3$ **5a** was obtained. RCY = 75% (Uncorrected for half-life). RCP = 97% (97%, after 24 h).

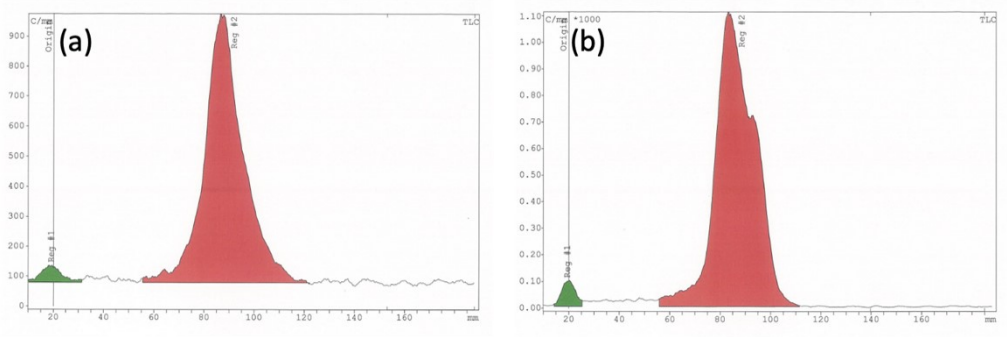

Fig. S4 Radio-TLC chromatogram of the purified compound **5a** obtained with the radio-TLC scanner. The horizontal axis represents the distance (mm) along the TLC plate between the observed peak (at 85 mm) and the original start line (at 20 mm) before elution. The vertical axis represents the intensity of radioactivity (counts/minutes). (a) Measurement immediately after purification (RCP 97%). (b) Measurement at 24 hours after purification (RCP 97%). TLC eluent: MeCN/H_2O (1:1).

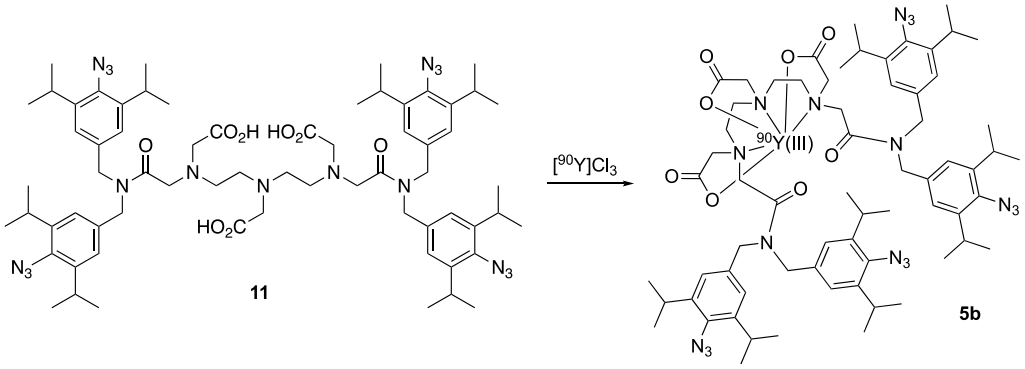

Synthesis of ^{90}Y-DTPA-4PhN$_3$ ***5b***: This reaction followed Procedure C. Upon reacting and purifying with 117 MBq of ^{90}Y, 110 MBq of ^{90}Y-DTPA-4PhN$_3$ **5b** was obtained. RCY = 94% (uncorrected for half-life). RCP = 99%.

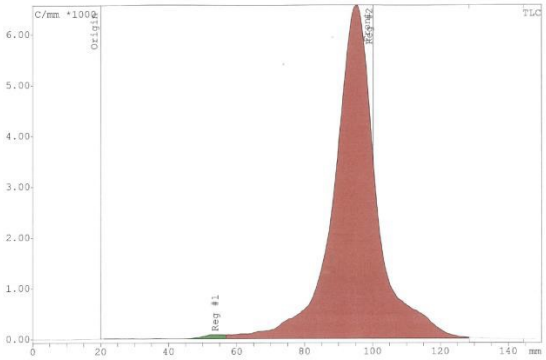

Fig. S5 Radio-TLC chromatogram of the purified compound **5b** obtained with the radio-TLC scanner. The horizontal axis represents the distance (mm) along the TLC plate between the observed peak (at 95 mm) and the original start line (at 20 mm) before elution. The vertical axis represents the intensity of radioactivity (counts/minutes). Measurement immediately after purification (RCP 99%). TLC eluent: MeCN/H_2O (1:1).

Animal experiments

The study involving the use of animals was conducted in compliance with the relevant regulations and standards after the experimental plan was designed following the Regulations on Safety Management of Biological Experiments of the study institution, Nihon Medi-Physics Co., Ltd. Research Center, and was reviewed and approved by the Biological Experiment Committee. For all injections and tumor measurements, mice were anesthetized with 1 – 4% isoflurane in oxygen at a 2.5 – 3.0 L/minute flow rate.

Statistics: All quantitative results are expressed as mean and standard deviation. Indicators of statistical significance were unpaired two-tailed Student's t-test or two-way analysis of variance (ANOVA) with Tukey's or Šidák correction for multiple comparisons analyses. All statistical analyses were performed using a GraphPad PRISM (version 9.5.1, GraphPad Software, Inc., California, USA). Statistical significance was defined as a *P*-value < 0.05.

Cell lines and reagents: A549 cells were purchased from the European collection of Authenticated Cell Cultures. They were cultured in an F-12K Nutrient mixture (Gibco) supplemented with 10% fetal bovine serum (FBS) (ATCC) and 1% penicillin-streptomycin (Gibco). The cells were then incubated at 37 °C in a 5% CO_2 humidified atmosphere.

A549-bearing mice xenograft models for SPECT studies: The A549 (human lung) cancer xenograft tumors were established in 4-week-old female nude mice (BALB/c-nu/nu, The Jackson Laboratory Japan, Inc.) by subcutaneous injection of 7.66 x 10^6 cells in 100 μL of cold 50% Matrigel in PBS into the right shoulder subcutaneous. Tumor growth was then monitored. The mice were kept in a controlled temperature(18–28 °C), salinity, and aeration room with sufficient food and water for 12 hours a day and 12 hours a night. After the tumor reached 200 – 350 mm^3 (25 days), the A549 tumor-bearing mice were ready for treatment studies.

A549-bearing mice xenograft models for Treatment studies: The A549 (human lung) cancer xenograft tumors were established in 4-week-old female nude mice (BALB/c-nu/nu, The Jackson Laboratory Japan, Inc.) by subcutaneous injection of 7.66 x 10^6 cells in 100 μL of cold 50% Matrigel in PBS into the right shoulder subcutaneous. Tumor growth was then monitored. The mice were kept in a controlled temperature(18–28 °C), salinity, and aeration room with sufficient food and water for 12 hours a day and 12 hours a night. After the tumor reached 50 – 150 mm^3 (10 days), the A549 tumor-bearing mice were ready for treatment studies.

SPECT studies

The mice selected for Single Photon Emission Computed Tomography (SPECT) imaging were divided into groups (*n* = 3 for each group) based on visual observation, ensuring no specific abnormalities and minimizing the differences in tumor volume and body weight averages among the groups. The mice were anesthetized, and ^{111}In-labeled compounds (10 MBq / 10 μL of 10% EtOH / saline) were administered into the tumor under 1–4% isoflurane anesthesia. SPECT and Computed Tomography (CT) imaging, each lasting approximately 30 minutes, were conducted at 1, 6, 24, 48, and 72 hours post-administration under 1–2% isoflurane anesthesia. SPECT and CT imaging were performed using the small-animal SPECT/CT system FX-3000 (Trifoil Imaging). From the composite images of SPECT and CT, the accumulation of ^{111}In-labeled compounds in the tumor and trunk was obtained in axial and coronal images using PMOD software (PMOD Technologies). Subsequently, image analysis was performed using AMIDE (AMIDE Development Team). The image analysis identified the positions of the tumor, muscles, heart, liver, and kidneys from the SPECT and CT composite images. Three-dimensional regions of interest [volume of interest (VOI)] were defined for each time point and tissue. Standardized uptake value (SUV) was calculated from the VOIs set at each time point and for each tissue. SUV is calculated as [radioactivity concentration in the volume of interest (VOI) (MBq/mL) / (administered radioactivity (MBq) / mouse body weight (g))].

Table S1 SPECT imaging and image reconstruction conditions.

Parameters	Conditions
Isotope/Energy	Indium-111/High-energy (220-270 keV)
Detector	Cadmium Zinc Telluride, 4-head
Collimator	MMP 952
Radius of rotation	50 mm
Field of view	60 mm
Scan-mode/degree	Tomography/180 degrees
Scan-time	32 minutes（240 seconds/projection, 8-projection）
Reconstruction-algorithm	3 dimensional - ordered subset expectation maximization method
Reconstruction-parameter	Iteration 4, Subsets 8

Table S2 CT imaging conditions.

Parameters	Conditions
Current/Voltage	450 μA/50 kV
Exposure time	230 mS
Magnification	1.5
Field of view	78.9 mm
Projection count	128 views
Frame averaged	1 frames/view

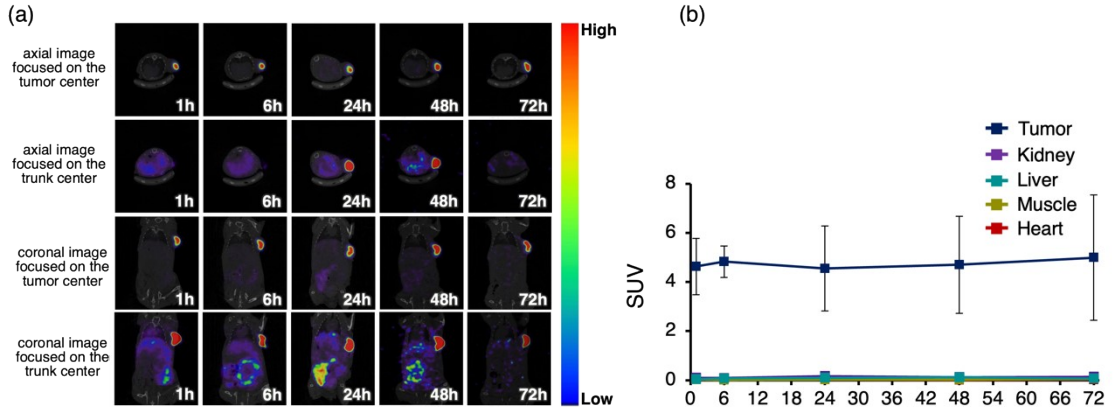

Fig. S6 (a) SPECT images were taken at various time points of mice administered with ^{111}In-DOTA-2PhN$_3$ **4**. Images were captured in both coronal and axial sections. Additionally, signal intensity thresholds were adjusted to depict the trunk or tumor in each section, resulting in four images in the figure. (b) The standardized uptake value (SUV) was calculated from SPECT images taken at each time point for 5 organs (*n* = 3). SUV is calculated as [radioactivity concentration in the volume of interest(VOI)) (MBq/mL) / (administered radioactivity (MBq) / mouse body weight (g))].

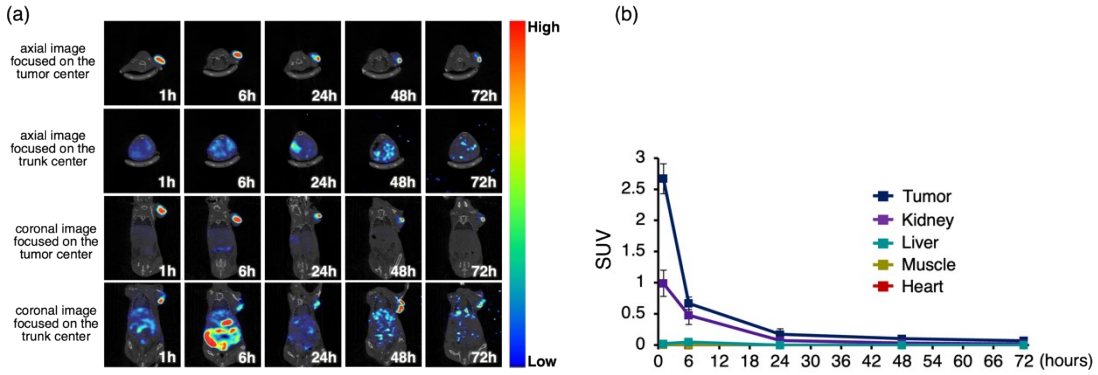

Fig. S7 (a) SPECT images were taken at various time points of mice administered with ^{111}In-DOTA-2PhH **S1**. Images were captured in both coronal and axial sections. Additionally, signal intensity thresholds were adjusted to depict the trunk or tumor in each section, resulting in four images in the figure. (b) The standardized uptake value (SUV) was calculated from SPECT images taken at each time point for 5 organs (*n* = 3). SUV is calculated as [radioactivity concentration in the volume of interest(VOI)) (MBq/mL) / (administered radioactivity (MBq) / mouse body weight (g))].

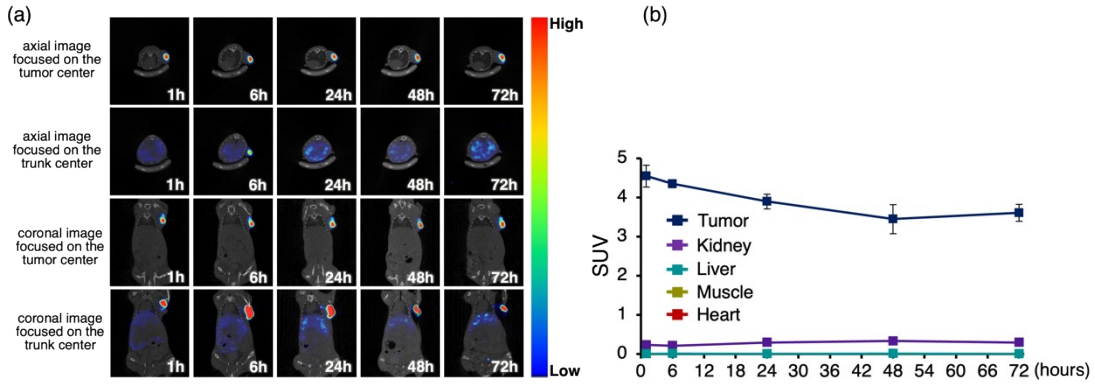

Fig. S8 (a) SPECT images were taken at various time points of mice administered with ^{111}In-DTPA-4PhN$_3$ **5a**. Images were captured in both coronal and axial sections. Additionally, signal intensity thresholds were adjusted to depict the trunk or tumor in each section, resulting in four images in the figure. (b) The standardized uptake value (SUV) was calculated from SPECT images taken at each time point for 5 organs (*n* = 3). SUV is calculated as [radioactivity concentration in the volume of interest(VOI) (MBq/mL) / (administered radioactivity (MBq) / mouse body weight (g))].

Table S3 Two-way ANOVA with Šidák correction was conducted to test the differences in tumor standardized uptake value (SUV) between the two groups (*n* = 3 for each group). The difference between the ^{111}In-DOTA-2PhN$_3$ **4**-treated group and the ^{111}In-DOTA-2PhH **S1**-treated group was significant starting from 6 hours post-administration, and this difference increased significantly throughout the entire experiment (see Fig. 2b in the manuscript). SUV is calculated as [radioactivity concentration in the volume of interest(VOI) (MBq/mL) / (administered radioactivity (MBq) / mouse body weight (g))] from SPECT images. n.s. = not significant, *P < 0.05, **P < 0.01, ***P < 0.001, ****P < 0.0001.

	^{111}In-DOTA-2PhN$_3$ **4** SUV (tumor)			^{111}In-DOTA-2PhH **S1** SUV (tumor)			Summary	Adjusted *P* value
Time (hours)	Mean ± SD			Mean ± SD				
1	4.63	±	1.15	2.67	±	0.24	n.s.	0.2876
6	4.83	±	0.64	0.67	±	0.10	**	0.0026
24	4.55	±	1.73	0.17	±	0.09	**	0.0015
48	4.70	±	1.97	0.10	±	0.02	***	0.0009
72	4.99	±	2.55	0.07	±	0.02	***	0.0004

Biodistribution studies

After the completion of SPECT imaging at the 72-hour time point, mice were euthanized under deep anesthesia with isoflurane inhalation (1.0 – 4.0%) and cardiac blood collection, followed by organ extraction (*n* = 3 for each group). Feces and urine were collected from the metabolic cage. The extracted organs included the tumor, heart, lungs, spleen, pancreas, stomach, small intestine, large intestine, ovaries, uterus, muscles, bones, liver, kidneys, whole brain, and the remaining whole body. The weights of the collected blood and organs (excluding feces and urine) were measured, and radioactivity was quantified to assess the distribution of radioactivity. Additionally, the radioactivity (count rate) obtained from the gamma well scintillation counting system was time-corrected to the time of ^{111}In administration. %ID for all tissues and %ID/g for organs excluding feces and urine were calculated.

Table S4 The distribution of radioactivity (%ID) in each tissue after SPECT imaging (*n* = 3) (see Fig. 2c in the manuscript).

	^{111}In-DOTA-2PhH **S1**			^{111}In-DOTA-2PhN$_3$ **4**			^{111}In-DTPA-4PhN$_3$ **5a**		
Tissue	Mean ± SD			Mean ± SD			Mean ± SD		
Tumor	1.543	±	0.551	3.269	±	1.179	53.11	±	3.937
Blood	0.005	±	0.002	0.014	±	0.002	0.306	±	0.101
Heart	0.014	±	0.004	0.022	±	0.003	0.044	±	0.014
Lung	0.040	±	0.006	0.057	±	0.014	0.079	±	0.013
Spleen	0.021	±	0.002	0.039	±	0.009	0.395	±	0.271
Pancreas	0.014	±	0.003	0.021	±	0.004	0.040	±	0.006
Stomach	0.016	±	0.007	0.028	±	0.009	0.052	±	0.022
Small intestine	0.241	±	0.062	0.405	±	0.038	0.753	±	0.220
Large intestine	0.197	±	0.082	0.584	±	0.212	0.598	±	0.030
Ovaries	0.001	±	0.000	0.002	±	0.002	0.001	±	0.000
Uterus	0.008	±	0.002	0.059	±	0.070	0.028	±	0.012
Muscle	0.003	±	0.000	0.009	±	0.003	0.011	±	0.003
Bone	0.006	±	0.002	0.009	±	0.002	0.039	±	0.009
Liver	0.823	±	0.141	0.768	±	0.061	6.837	±	0.764
Kidney	0.118	±	0.014	0.244	±	0.041	0.380	±	0.086
Whole brain	0.001	±	0.000	0.003	±	0.001	0.014	±	0.006
Remained whole body	0.873	±	0.123	3.408	±	0.321	21.13	±	3.652
Urine	9.128	±	6.284	9.961	±	2.823	0.797	±	0.645
Feces	86.95	±	5.991	81.10	±	1.554	15.38	±	0.473

Table S5 The distribution of radioactivity (%ID/g) in each tissue after SPECT imaging (n = 3).

	^{111}In-DOTA-2PhH **S1**			^{111}In-DOTA-2PhN_3 **4**			^{111}In-DTPA-4PhN_3 **5a**		
Tissue	Mean ± SD			Mean ± SD			Mean ± SD		
Tumor	4.437	±	1.464	13.79	±	7.495	146.6	±	28.38
Blood	0.006	±	0.001	0.020	±	0.001	0.387	±	0.155
Heart	0.134	±	0.046	0.216	±	0.016	0.412	±	0.155
Lung	0.338	±	0.071	0.455	±	0.055	0.635	±	0.150
Spleen	0.360	±	0.132	0.612	±	0.124	5.847	±	2.929
Pancreas	0.091	±	0.040	0.164	±	0.013	0.273	±	0.079
Stomach	0.070	±	0.069	0.100	±	0.048	0.124	±	0.043
Small intestine	0.261	±	0.150	0.389	±	0.015	0.650	±	0.261
Large intestine	0.333	±	0.309	0.523	±	0.267	0.457	±	0.103
Ovaries	0.224	±	0.123	0.857	±	0.794	0.685	±	0.529
Uterus	0.375	±	0.140	1.345	±	0.933	0.824	±	0.249
Muscle	0.038	±	0.007	0.089	±	0.019	0.126	±	0.043
Bone	0.079	±	0.013	0.152	±	0.014	0.463	±	0.101
Liver	0.890	±	0.435	0.771	±	0.152	6.342	±	0.304
Kidney	0.421	±	0.108	0.867	±	0.082	1.364	±	0.435
Whole brain	0.004	±	0.001	0.006	±	0.001	0.039	±	0.023
Remained whole body	0.077	±	0.020	0.282	±	0.015	1.722	±	0.384

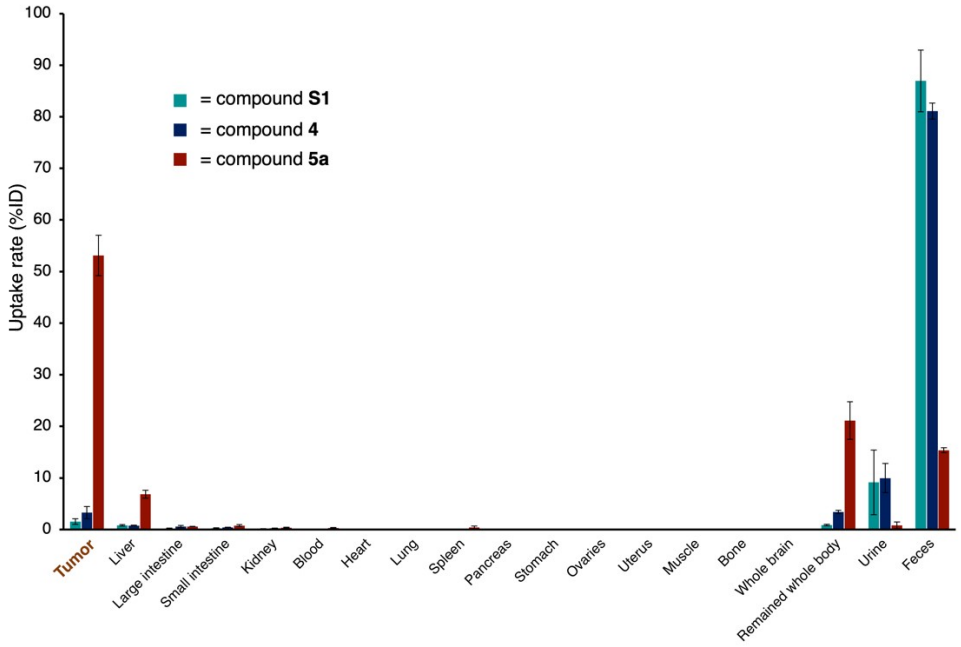

Fig. S9 Biodistribution (%ID) of **S1**, **4**, and **5a** in the xenograft mice 72 hours after the corresponding compounds were administered intratumorally (*n* = 3) (see also Fig. 2c in the manuscript).

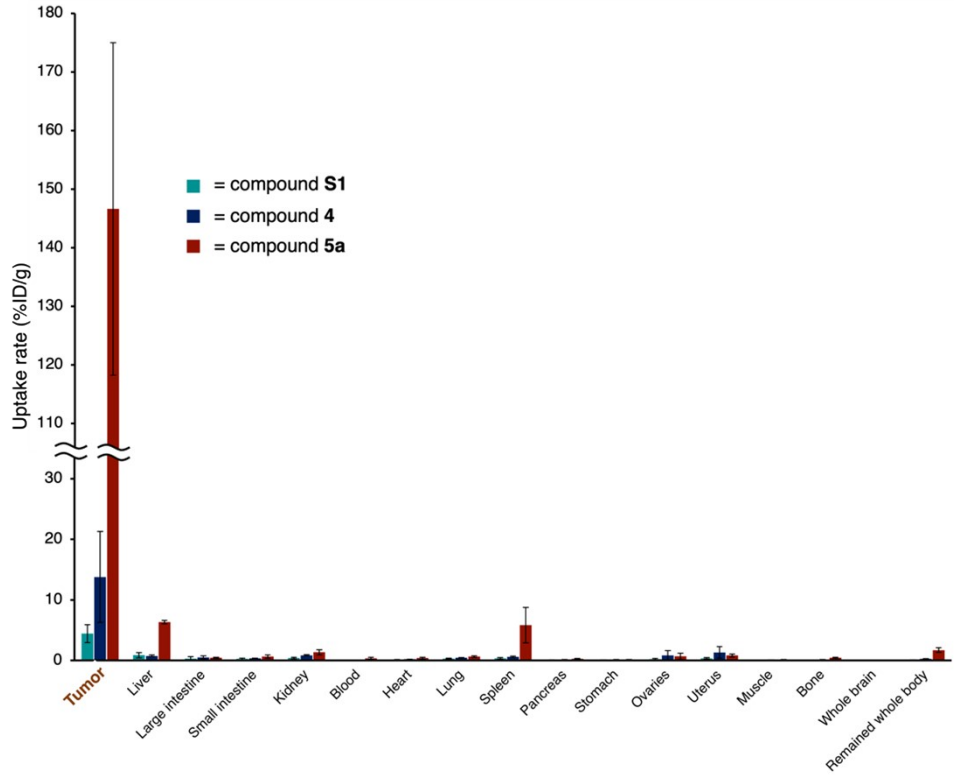

Fig. S10 Biodistribution (%ID/g) of **S1**, **4**, and **5a** in the xenograft mice 72 hours after the corresponding compounds were administered intratumorally (*n* = 3).

Table S6 The cell-based assay was conducted to determine the effectiveness of cellular uptake of $[^{111}In]Cl_3$ and compound **5a** into two cancer cell lines – PANC-1 cells and B16 cells. For both cell lines, 1 x 10^6 and 5 x 10^6 cells were used. The cells were incubated with 1.5 - 1.8 MBq of $[^{111}In]Cl_3$ or compound **5a** for 30 minutes at room temperature. After labeling, the radioactive amounts in the cell pellet or supernatant were measured using a dose calibrator immediately after labeling and after washing. PANC-1 = human pancreas

Cell line (Cell number)	Loading	After labeling			After washing		
		Cell pellet, CP (MBq)	Supernatant, S (MBq)	Uptake ratio CP/(CP+S) %	Cell pellet, CP (MBq)	Supernatant, S (MBq)	Uptake ratio CP/(CP+S) %
PANC-1 (1 x 10^6)	$[^{111}In]Cl_3$	0.06	0.81	6.6%	0.04	0.99	3.4%
	Compound **5a**	0.26	0.85	**23.0%**	0.06	1.09	**5.2%**
PANC-1 (5 x 10^6)	$[^{111}In]Cl_3$	0.06	0.87	6.8%	0.04	1.00	3.5%
	Compound **5a**	0.31	0.87	**26.3%**	0.06	1.11	**5.3%**
B16 (1 x 10^6)	$[^{111}In]Cl_3$	0.19	1.01	15.9%	0.06	1.13	5.1%
	Compound **5a**	0.31	0.92	**25.0%**	0.14	1.09	**11.0%**
B16 (5 x 10^6)	$[^{111}In]Cl_3$	0.23	1.01	18.6%	0.07	1.16	5.5%
	Compound **5a**	0.53	0.81	**39.6%**	0.32	1.02	**24.1%**

Cancer treatment studies

The mice selected for treatment studies were divided into four groups (*n* = 6 for each group) based on visual observation, ensuring no specific abnormalities and minimizing the differences in tumor volume and body weight averages among the groups. Four groups of mice were injected intratumorally with a solution of 0 MBq (vehicle), 0.1, 0.5, and 2.5 MBq of ^{90}Y-DTPA-4PhN$_3$ **5b** dissolved in 10 μL of 10% EtOH/saline (20 μM DTPA-4PhN$_3$ **11**), respectively. The mice's tumor volume and body weight were recorded within a specific period using the equation $V = W^2 \times L / 2$, where W and L represented the minor and major lengths of the tumor, respectively. After the completion of the measurement of tumor volume at the 33-day time point, mice were euthanized under deep anesthesia with isoflurane inhalation (1.0 – 4.0%) and bloodletting, followed by organ extraction. The extracted organs included the tumor, heart, lungs, spleen, pancreas, liver, kidneys, and the remaining whole body. The weight of each organ removed from the mice was measured. The relative weight of the organs in each group was calculated by comparing the weight of the organs in the vehicle group.

Table S7 Two-way ANOVA with Tukey's correction was performed to test group tumor growth differences (*n* = 6) (see manuscript Fig. 3a). The difference between the vehicle-treated and ^{90}Y-DTPA-4PhN$_3$ **5b**-treated groups was significant starting 13 days after treatment. The considerable increase continued throughout the experiment. Vehicle = Saline (10% EtOH, 20 μM DTPA-4PhN$_3$ **11**). n.s. = not significant, *P < 0.05, **P < 0.01, ***P < 0.001, ****P < 0.0001.

Post-treatment (days)	Vehicle vs. ^{90}Y-DTPA-4PhN$_3$ **5b** (0.1MBq)		Vehicle vs. ^{90}Y-DTPA-4PhN$_3$ **5b** (0.5MBq)		Vehicle vs. ^{90}Y-DTPA-4PhN$_3$ **5b** (2.5MBq)	
	Summary	Adjusted *P* value	Summary	Adjusted *P* value	Summary	Adjusted *P* value
0	n.s.	>0.9999	n.s.	>0.9999	n.s.	>0.9999
4	n.s.	0.8886	n.s.	0.5330	n.s.	0.4283
7	n.s.	0.9372	n.s.	0.4593	n.s.	0.4934
11	n.s.	0.8757	n.s.	0.2191	n.s.	0.1364
13	n.s.	0.3563	*	0.0186	*	0.0199
18	n.s.	0.1176	****	<0.0001	****	<0.0001
21	*	0.0268	****	<0.0001	****	<0.0001
25	*	0.0224	****	<0.0001	****	<0.0001
28	***	0.0005	****	<0.0001	****	<0.0001

Table S8 Two-way ANOVA with Tukey's correction was performed to test group tumor growth differences (*n* = 6) (see manuscript Fig. 3a). The difference between the ^{90}Y-DTPA-4PhN$_3$ **5b** 0.1 MBq-treated group and the 0.5 and 2.5 MBq-treated groups was significant starting 18 days after treatment. Vehicle = Saline (10% EtOH, 20 μM DTPA-4PhN$_3$ **11**). n.s. = not significant, *P < 0.05, **P < 0.01, ***P < 0.001, ****P < 0.0001.

Post-treatment (days)	^{90}Y-DTPA-4PhN$_3$ **5b** (0.1MBq) vs. ^{90}Y-DTPA-4PhN$_3$ **5b** (0.5MBq)		^{90}Y-DTPA-4PhN$_3$ **5b** (0.1MBq) vs. ^{90}Y-DTPA-4PhN$_3$ **5b** (2.5MBq)		^{90}Y-DTPA-4PhN$_3$ **5b** (0.5MBq) vs. ^{90}Y-DTPA-4PhN$_3$ **5b** (2.5MBq)	
	Summary	Adjusted *P* value	Summary	Adjusted *P* value	Summary	Adjusted *P* value
0	n.s.	>0.9999	n.s.	0.9996	n.s.	0.9996
4	n.s.	0.9229	n.s.	0.8552	n.s.	0.9983
7	n.s.	0.8127	n.s.	0.8403	n.s.	>0.9999
11	n.s.	0.6413	n.s.	0.4913	n.s.	0.9953
13	n.s.	0.5596	n.s.	0.5738	n.s.	>0.9999
18	*	0.0312	**	0.0031	n.s.	0.8788
21	***	0.0009	****	<0.0001	n.s.	0.6162
25	****	<0.0001	****	<0.0001	n.s.	0.3069
28	****	<0.0001	****	<0.0001	n.s.	0.1100

Table S9 Two-way ANOVA with Tukey's correction was performed to test group relative body weight change differences (*n* = 6) (see manuscript Fig. 3b). There were no combinations for which significant differences were identified. Vehicle = Saline (10% EtOH, 20 μM DTPA-4PhN$_3$ **11**). n.s. = not significant, *P < 0.05, **P < 0.01, ***P < 0.001, ****P < 0.0001.

Post-treatment (days)	Vehicle vs. ^{90}Y-DTPA-4PhN$_3$ **5b** (0.1MBq)		Vehicle vs. ^{90}Y-DTPA-4PhN$_3$ **5b** (0.5MBq)		Vehicle vs. ^{90}Y-DTPA-4PhN$_3$ **5b** (2.5MBq)	
	Summary	Adjusted *P* value	Summary	Adjusted *P* value	Summary	Adjusted *P* value
0	n.s.	0.3198	n.s.	0.7767	n.s.	0.5053
4	n.s.	0.1217	n.s.	0.9389	n.s.	0.9782
7	n.s.	0.2354	n.s.	0.9432	n.s.	0.7479
11	n.s.	0.1304	n.s.	0.6088	n.s.	0.5027
13	n.s.	0.3456	n.s.	0.9831	n.s.	0.6662
18	n.s.	0.1960	n.s.	0.8566	n.s.	0.5629
21	n.s.	0.2746	n.s.	0.9654	n.s.	0.9090
25	n.s.	0.5133	n.s.	0.9988	n.s.	0.9020
28	n.s.	0.2889	n.s.	>0.9999	n.s.	0.7368

Table S10 Two-way ANOVA with Tukey's correction was performed to test group relative body weight change differences (*n* = 6) (see manuscript Fig. 3b). There were no combinations for which significant differences were identified. Vehicle = Saline (10% EtOH, 20 μM DTPA-4PhN$_3$ **11**). n.s. = not significant, *P < 0.05, **P < 0.01, ***P < 0.001, ****P < 0.0001.

Post-treatment (days)	^{90}Y-DTPA-4PhN$_3$ **5b** (0.1MBq) vs. ^{90}Y-DTPA-4PhN$_3$ **5b** (0.5MBq)		^{90}Y-DTPA-4PhN$_3$ **5b** (0.1MBq) vs. ^{90}Y-DTPA-4PhN$_3$ **5b** (2.5MBq)		^{90}Y-DTPA-4PhN$_3$ **5b** (0.5MBq) vs. ^{90}Y-DTPA-4PhN$_3$ **5b** (2.5MBq)	
	Summary	Adjusted *P* value	Summary	Adjusted *P* value	Summary	Adjusted *P* value
0	n.s.	0.8717	n.s.	0.9886	n.s.	0.9713
4	n.s.	0.3571	n.s.	0.2677	n.s.	0.9981
7	n.s.	0.5454	n.s.	0.8109	n.s.	0.9713
11	n.s.	0.7732	n.s.	0.8585	n.s.	0.9983
13	n.s.	0.5656	n.s.	0.9527	n.s.	0.8671
18	n.s.	0.6316	n.s.	0.9020	n.s.	0.9574
21	n.s.	0.5427	n.s.	0.6675	n.s.	0.9973
25	n.s.	0.6074	n.s.	0.8995	n.s.	0.9495
28	n.s.	0.3111	n.s.	0.8754	n.s.	0.7625

Table S11 Two-way ANOVA with Tukey's correction was performed to test group differences for each relative organ weight (*n* = 6) (see manuscript Fig. 3c). There was a significant difference in tumor and spleen between the vehicle group and the ^{90}Y-DTPA-4PhN$_3$ **5b** group. Vehicle = Saline (10% EtOH, 20 μM DTPA-4PhN$_3$ **11**). n.s. = not significant, *P < 0.05, **P < 0.01, ***P < 0.001, ****P < 0.0001.

organs	Vehicle vs. ^{90}Y-DTPA-4PhN$_3$ **5b** (0.1MBq)		Vehicle vs. ^{90}Y-DTPA-4PhN$_3$ **5b** (0.5MBq)		Vehicle vs. ^{90}Y-DTPA-4PhN$_3$ **5b** (2.5MBq)	
	Summary	Adjusted *P* value	Summary	Adjusted *P* value	Summary	Adjusted *P* value
Tumor	n.s.	0.4467	****	<0.0001	****	<0.0001
Heart	n.s.	0.3899	n.s.	0.6319	n.s.	0.5754
Lung	n.s.	0.7478	n.s.	0.8756	n.s.	0.8532
Spleen	****	<0.0001	*	0.0177	**	0.0036
Pancreas	n.s.	0.3428	n.s.	0.6297	n.s.	0.3428
Liver	n.s.	0.5052	n.s.	0.3992	n.s.	0.1357
Kidney	n.s.	0.6667	n.s.	0.8522	n.s.	0.6559

Table S12 Two-way ANOVA with Tukey's correction was performed to test group differences for each relative organ weight (*n* = 6) (see manuscript Fig. 3c). In the comparison between the ^{90}Y-DTPA-4PhN$_3$ **5b** treatment groups, there was a significant difference only in the tumor. Vehicle = Saline (10% EtOH, 20 μM DTPA-4PhN$_3$ **11**). n.s. = not significant, *P < 0.05, **P < 0.01, ***P < 0.001, ****P < 0.0001.

organs	^{90}Y-DTPA-4PhN$_3$ **5b** (0.1MBq) vs. ^{90}Y-DTPA-4PhN$_3$ **5b** (0.5MBq)		^{90}Y-DTPA-4PhN$_3$ **5b** (0.1MBq) vs. ^{90}Y-DTPA-4PhN$_3$ **5b** (2.5MBq)		^{90}Y-DTPA-4PhN$_3$ **5b** (0.5MBq) vs. ^{90}Y-DTPA-4PhN$_3$ **5b** (2.5MBq)	
	Summary	Adjusted *P* value	Summary	Adjusted *P* value	Summary	Adjusted *P* value
Tumor	****	<0.0001	****	<0.0001	n.s.	0.1649
Heart	n.s.	0.9795	n.s.	0.9903	n.s.	0.9997
Lung	n.s.	0.9944	n.s.	0.9971	n.s.	>0.9999
Spleen	n.s.	0.3694	n.s.	0.6822	n.s.	0.9569
Pancreas	n.s.	0.9648	n.s.	>0.9999	n.s.	0.9648
Liver	n.s.	0.9981	n.s.	0.8644	n.s.	0.9312
Kidney	n.s.	0.9872	n.s.	>0.9999	n.s.	0.9852

^{1}H-NMR in $CDCl_3$

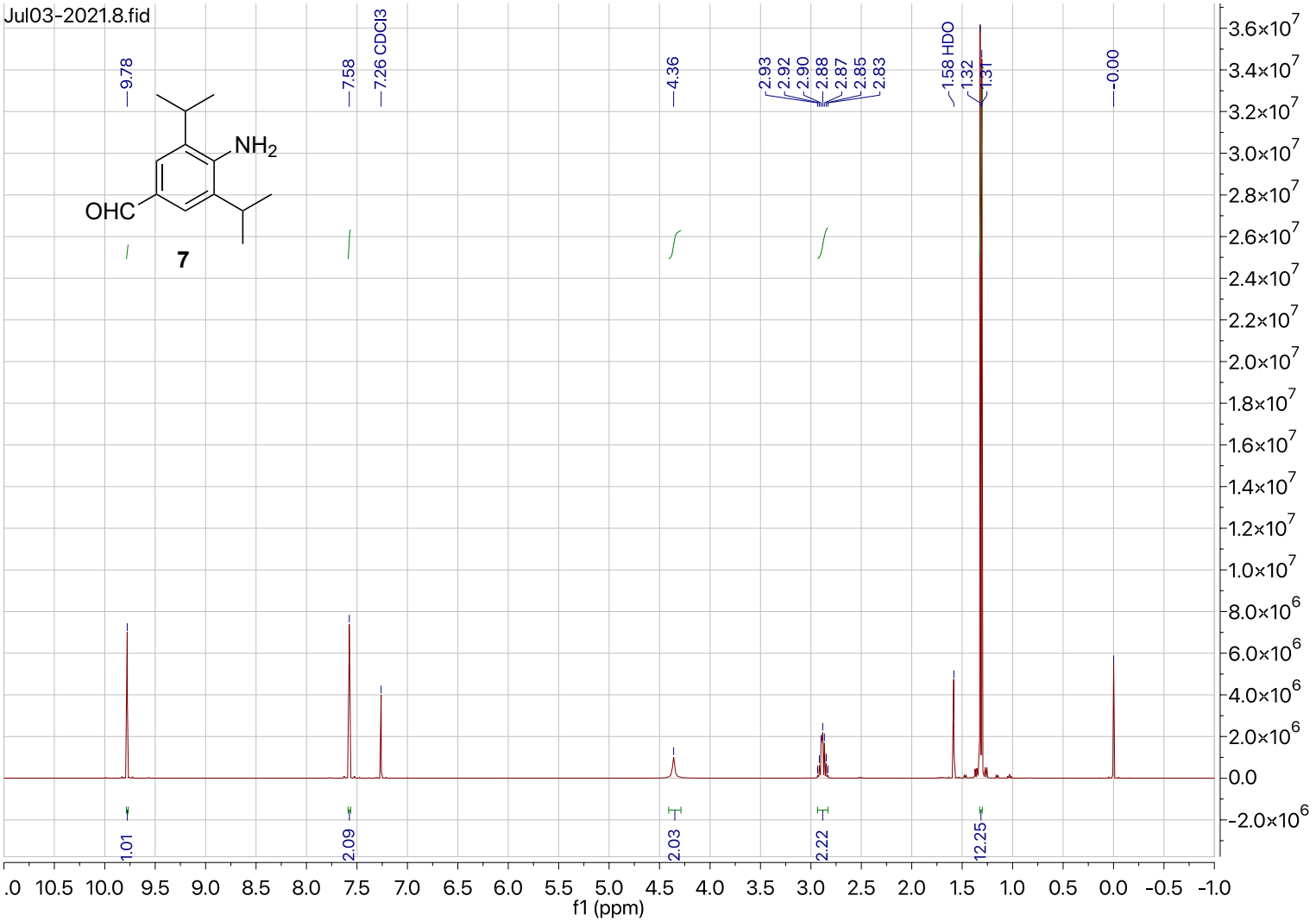

^{13}C-NMR in $CDCl_3$

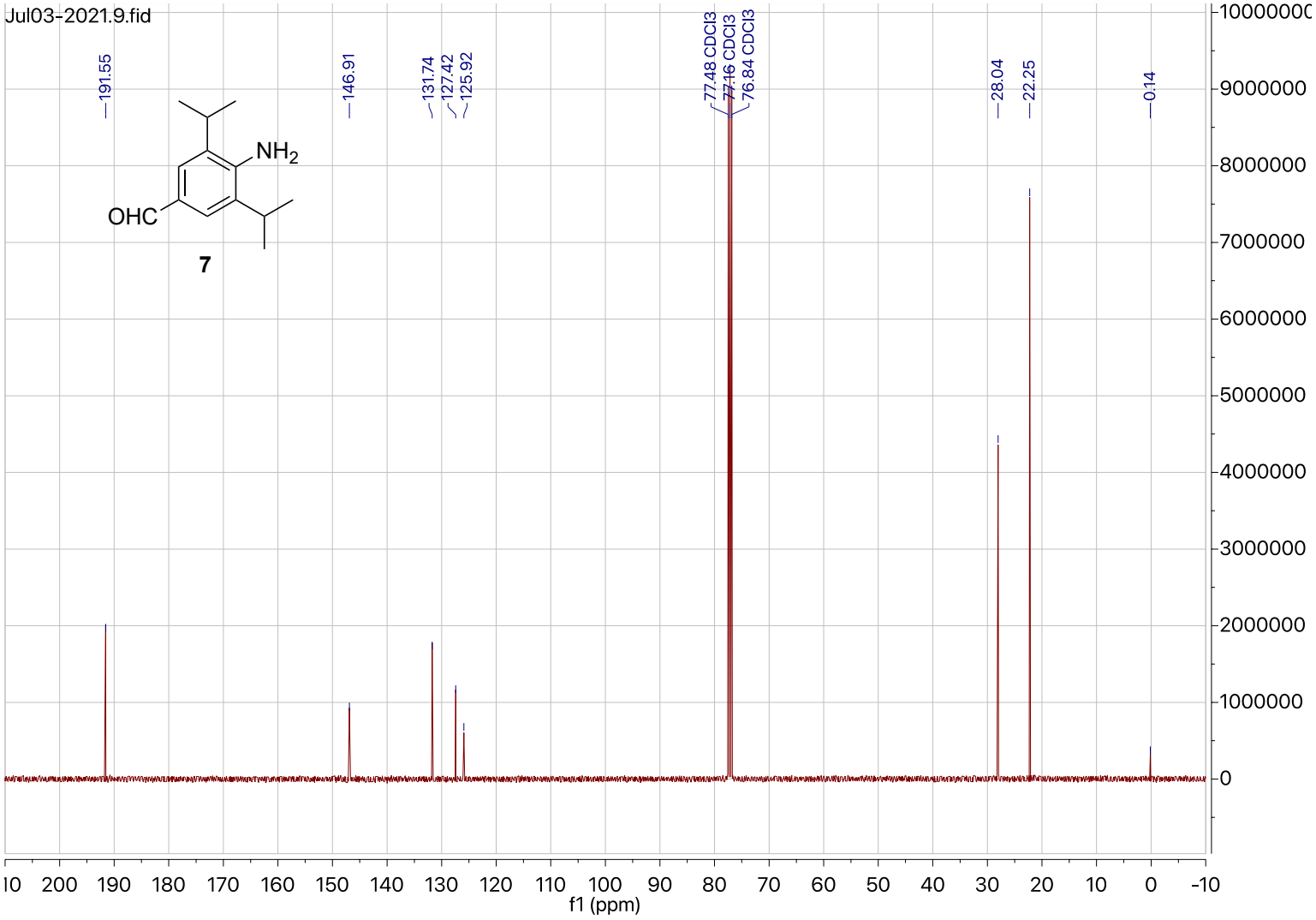

Mass Spectrum SmartFormula Report

Analysis Info

Analysis Name	D:\Data\User Data\Ode\000820_1-91_01_18224.d	Acquisition Date	2023/10/01 21:18:56
Method	lcms_esi_pos_low.m	Operator	BDAL@DE
Sample Name	000820	Instrument	micrOTOF II 8213750.10448
Comment			

Acquisition Parameter

Source Type	ESI	Ion Polarity	Positive	Set Nebulizer	3.0 Bar
Focus	Not active			Set Dry Heater	200 • ‹C
Scan Begin	50 m/z	Set Capillary	4500 V	Set Dry Gas	10.0 l/min
Scan End	2000 m/z	Set End Plate Offset	-500 V	Set Divert Valve	Waste

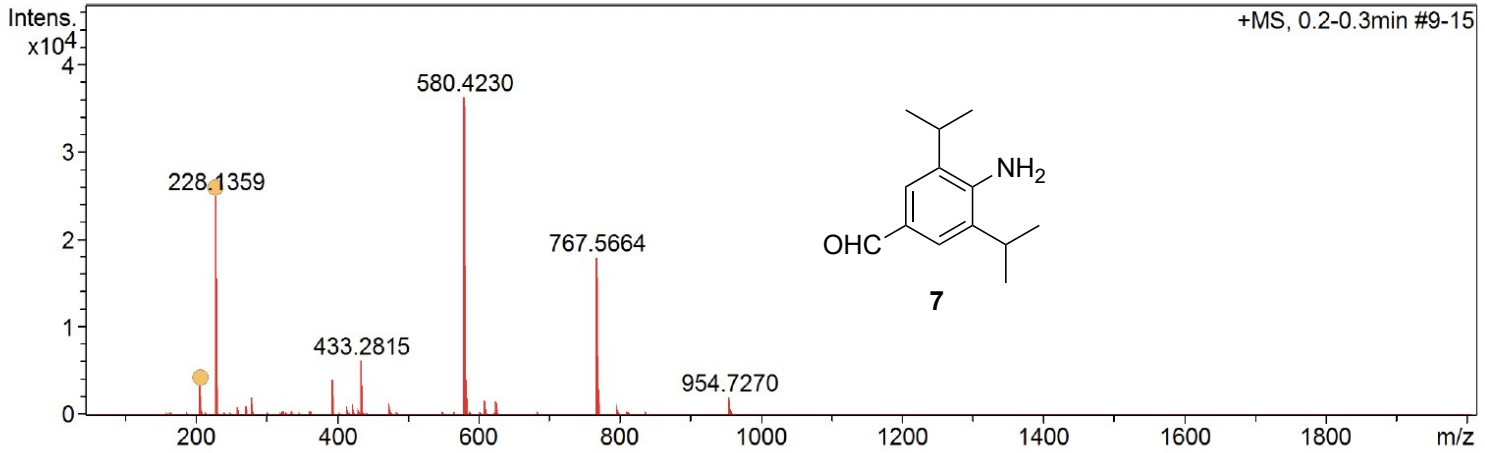

Meas. m/z	#	Ion Formula	m/z	err [ppm]	mSigma	# mSigma	Score	rdb	e• P Conf	N-Rule
206.1523	1	C13H20NO	206.1539	7.8	10.4	1	100.00	4.5	even	ok
228.1359	1	C13H19NNaO	228.1359	-0.1	8.3	1	100.00	4.5	even	ok

^{1}H-NMR in $CDCl_3$

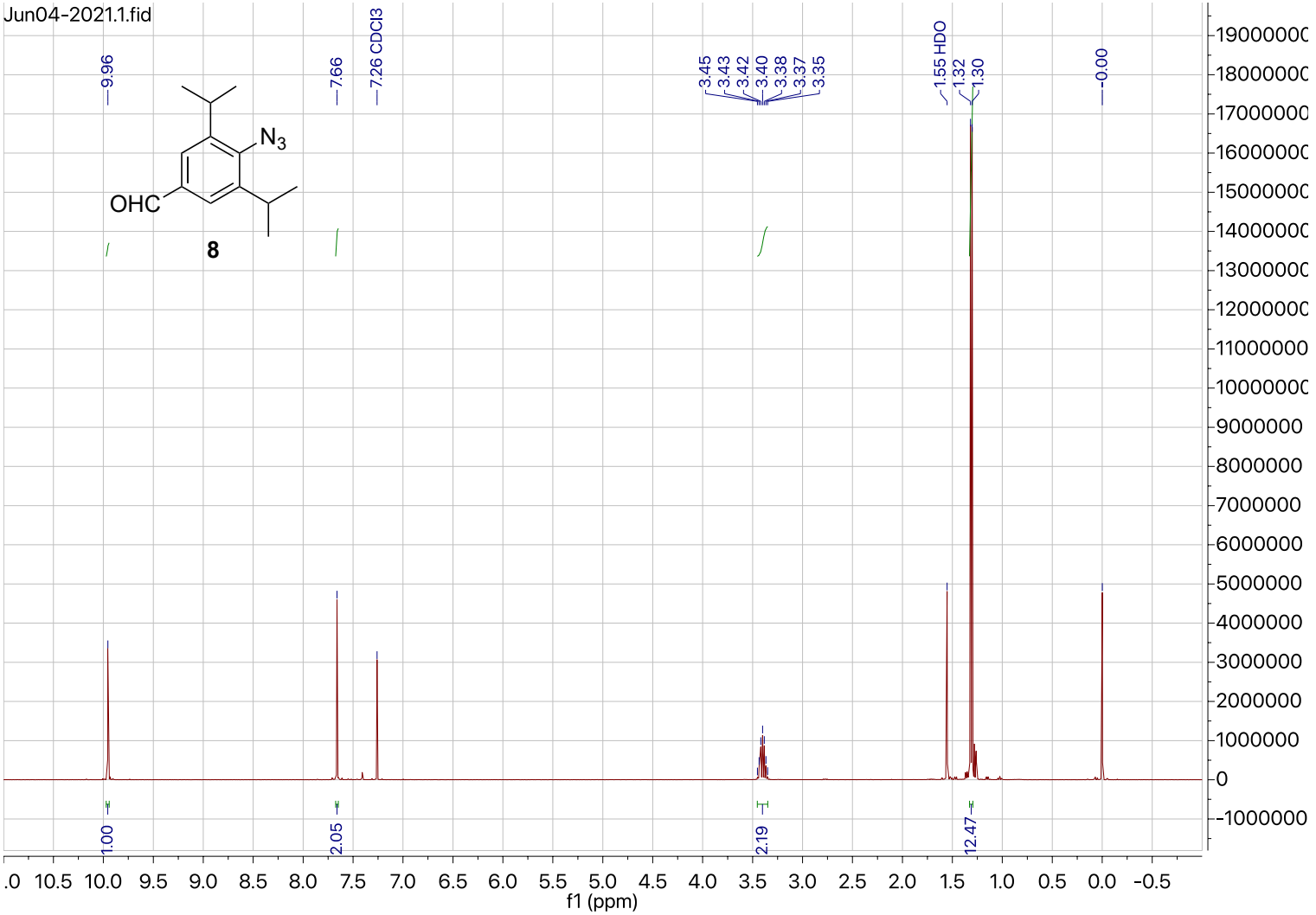

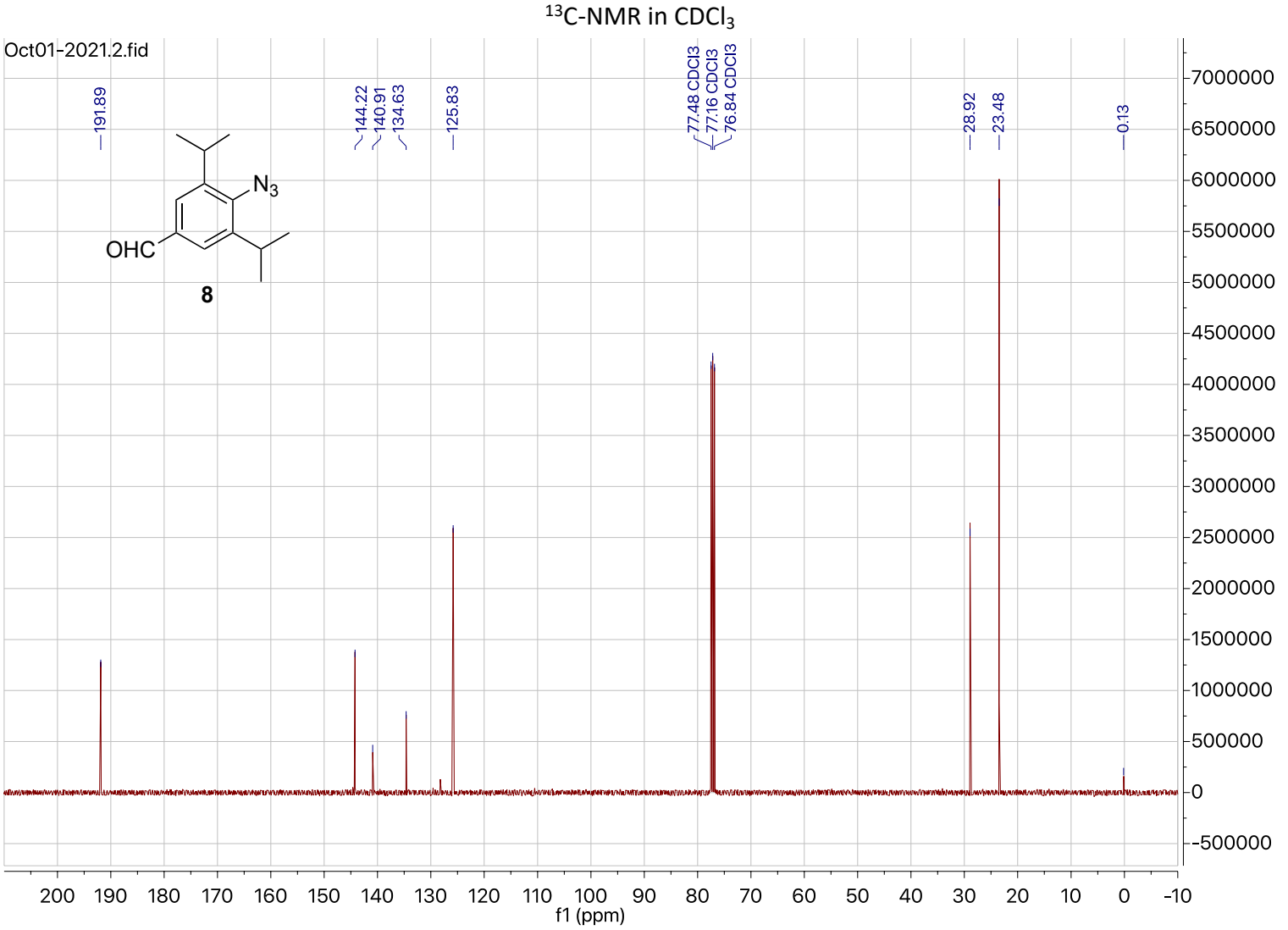
^{13}C-NMR in $CDCl_3$
Oct01-2021.2.fid
191.89
144.22
140.91
134.63
125.83
77.48 CDCl3
77.16 CDCl3
76.84 CDCl3
28.92
23.48
0.13
N_3
OHC
8
7000000
6500000
6000000
5500000
5000000
4500000
4000000
3500000
3000000
2500000
2000000
1500000
1000000
500000
0
-500000
200 190 180 170 160 150 140 130 120 110 100 90 80 70 60 50 40 30 20 10 0 -10
f1 (ppm)

Mass Spectrum SmartFormula Report

Analysis Info

Analysis Name	D:\Data\User Data\Ode\000832_1-91_01_18964.d	Acquisition Date	2023/11/25 15:00:58
Method	lcms_esi_pos_low.m	Operator	BDAL@DE
Sample Name	000832	Instrument	micrOTOF II 8213750.10448
Comment			

Acquisition Parameter

Source Type	ESI	Ion Polarity	Positive	Set Nebulizer	3.0 Bar
Focus	Not active			Set Dry Heater	200 • ‹C
Scan Begin	50 m/z	Set Capillary	4500 V	Set Dry Gas	10.0 l/min
Scan End	2000 m/z	Set End Plate Offset	-500 V	Set Divert Valve	Waste

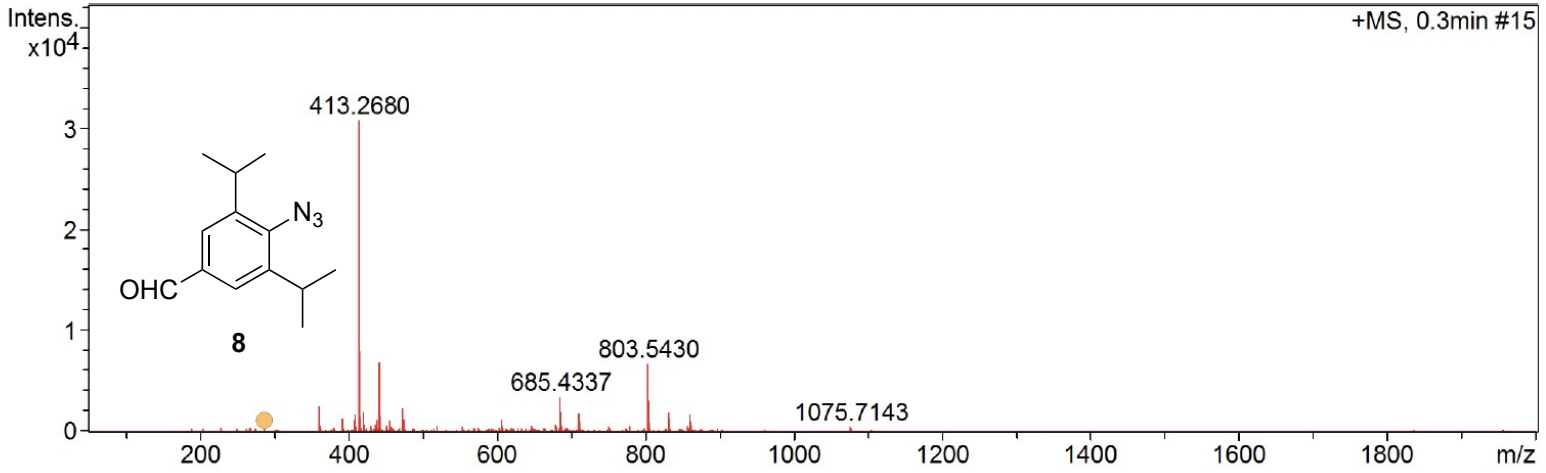

Meas. m/z	#	Ion Formula	m/z	err [ppm]	mSigma	# mSigma	Score	rdb	e• P Conf	N-Rule
286.1524	1	C14H21N3NaO2	286.1526	0.6	25.7	1	100.00	5.5	even	ok

^{1}H-NMR in $CDCl_3$

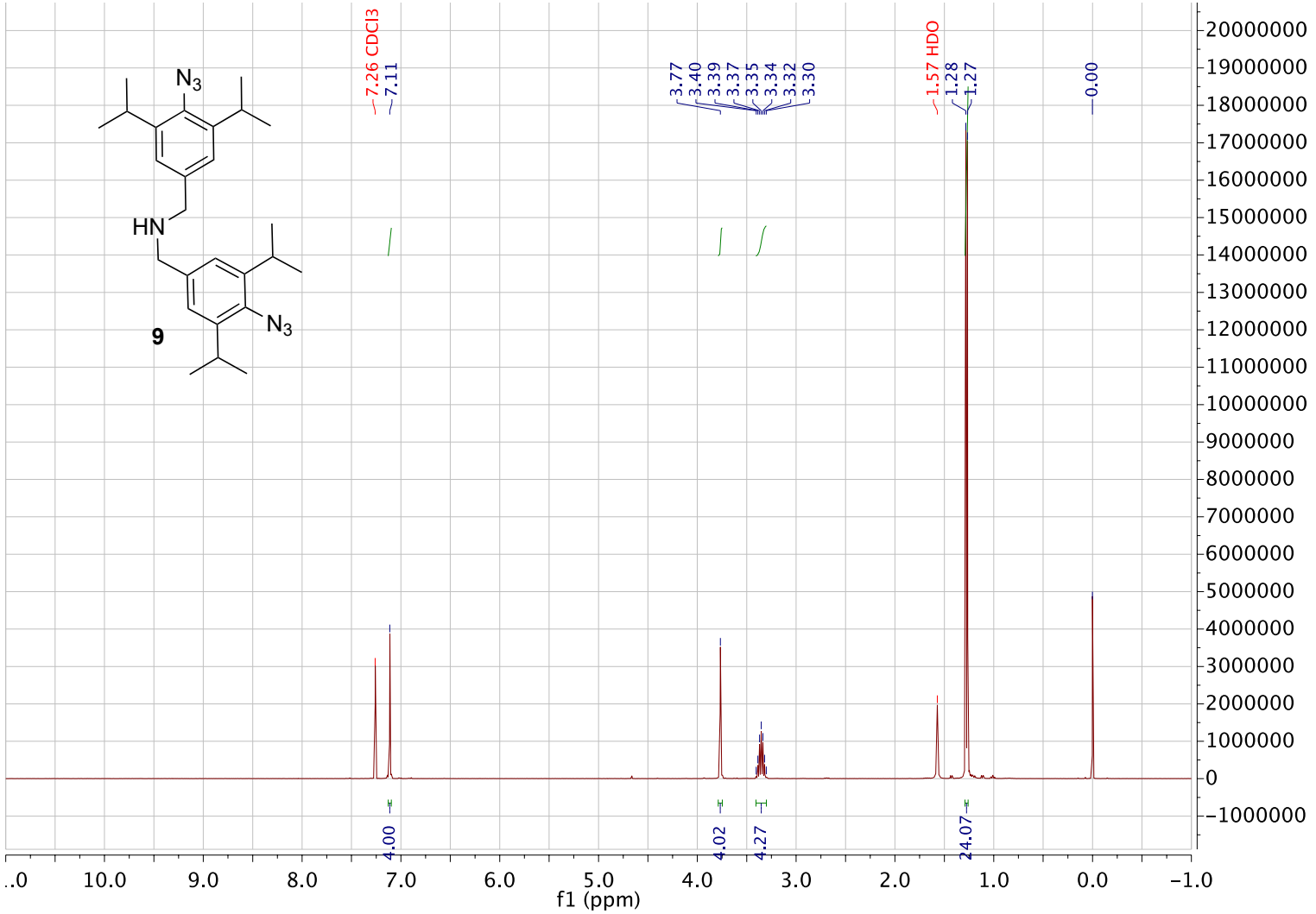

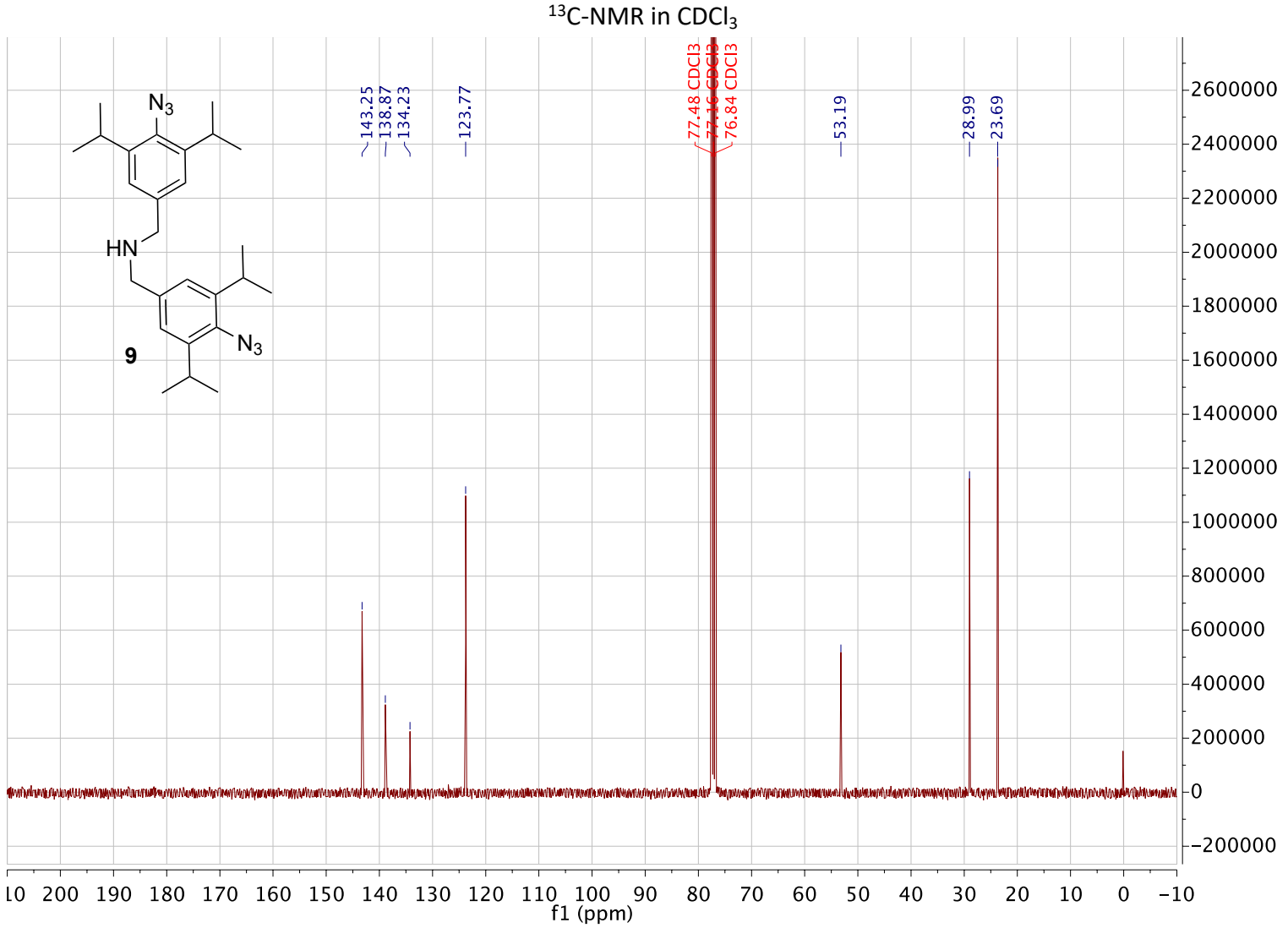
^{13}C-NMR in $CDCl_3$
N3
HN
N3
9
143.25
138.87
134.23
123.77
77.48 CDCl3
77.16 CDCl3
76.84 CDCl3
53.19
28.99
23.69
2600000
2400000
2200000
2000000
1800000
1600000
1400000
1200000
1000000
800000
600000
400000
200000
0
−200000
f1 (ppm)

Mass Spectrum SmartFormula Report

Analysis Info

Analysis Name	D:\Data\User Data\Ode\000829_1-100_01_18233.d	Acquisition Date	2023/10/01 21:52:31
Method	lcms_esi_pos_low.m	Operator	BDAL@DE
Sample Name	000829	Instrument	micrOTOF II 8213750.10448
Comment			

Acquisition Parameter

Source Type	ESI	Ion Polarity	Positive	Set Nebulizer	3.0 Bar
Focus	Not active			Set Dry Heater	200 • ‹C
Scan Begin	50 m/z	Set Capillary	4500 V	Set Dry Gas	10.0 l/min
Scan End	2000 m/z	Set End Plate Offset	-500 V	Set Divert Valve	Waste

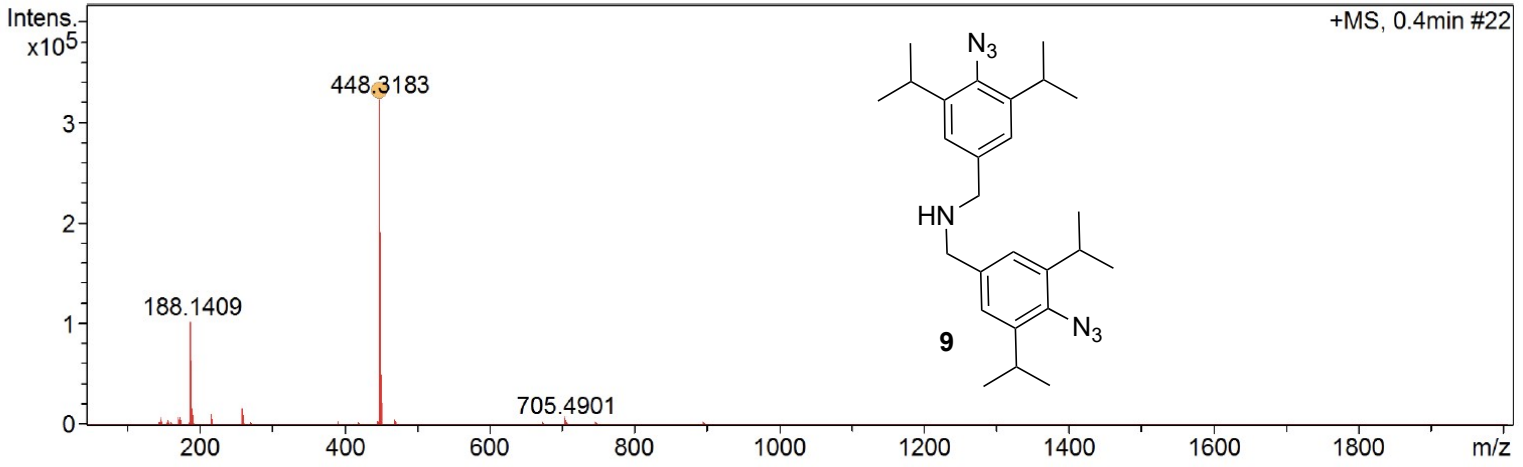

Meas. m/z	#	Ion Formula	m/z	err [ppm]	mSigma	# mSigma	Score	rdb	e• P Conf	N-Rule
448.3183	1	C26H38N7	448.3183	0.0	8.9	1	100.00	11.5	even	ok

^{1}H-NMR in $CDCl_3$

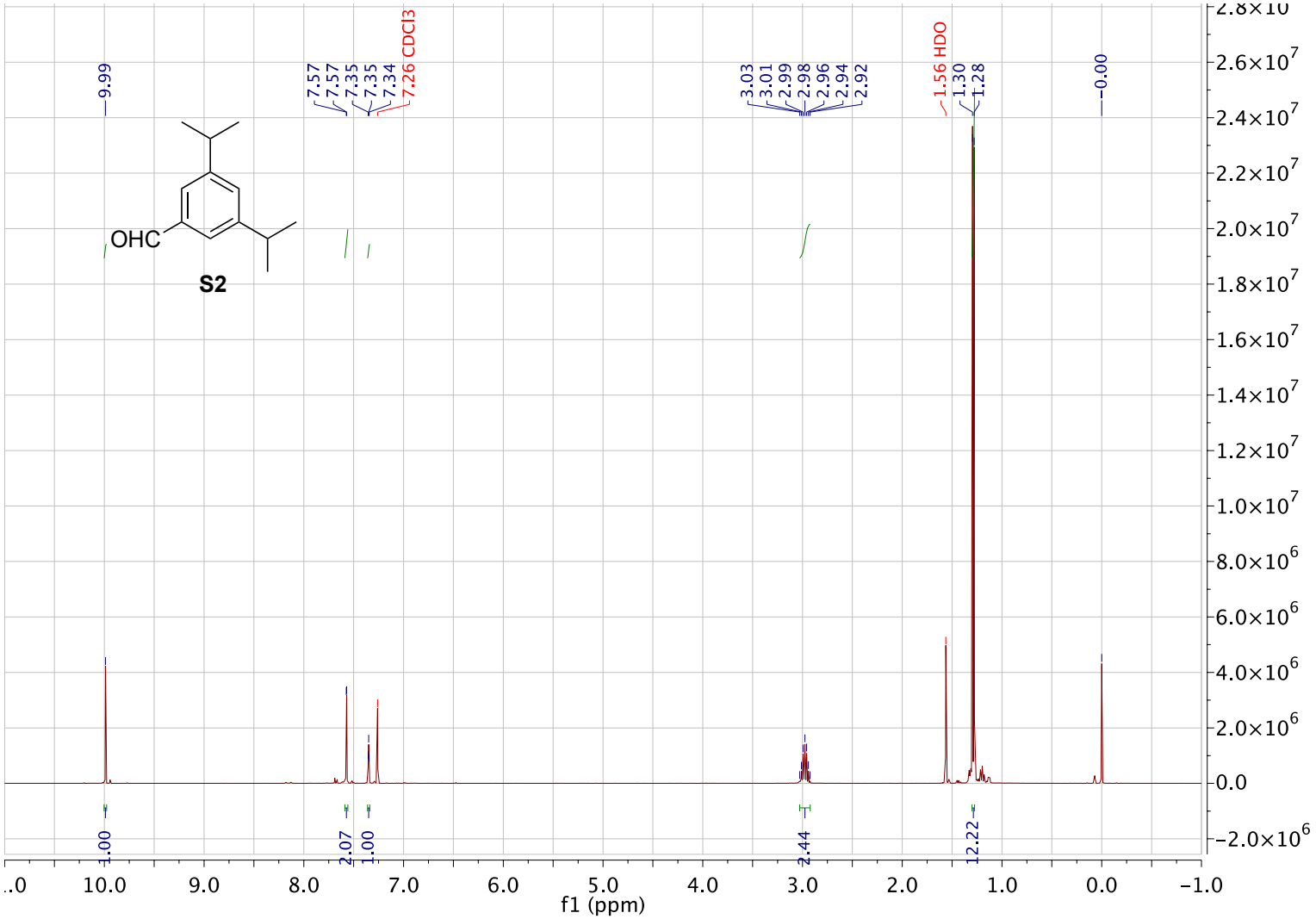

^{13}C-NMR in $CDCl_3$

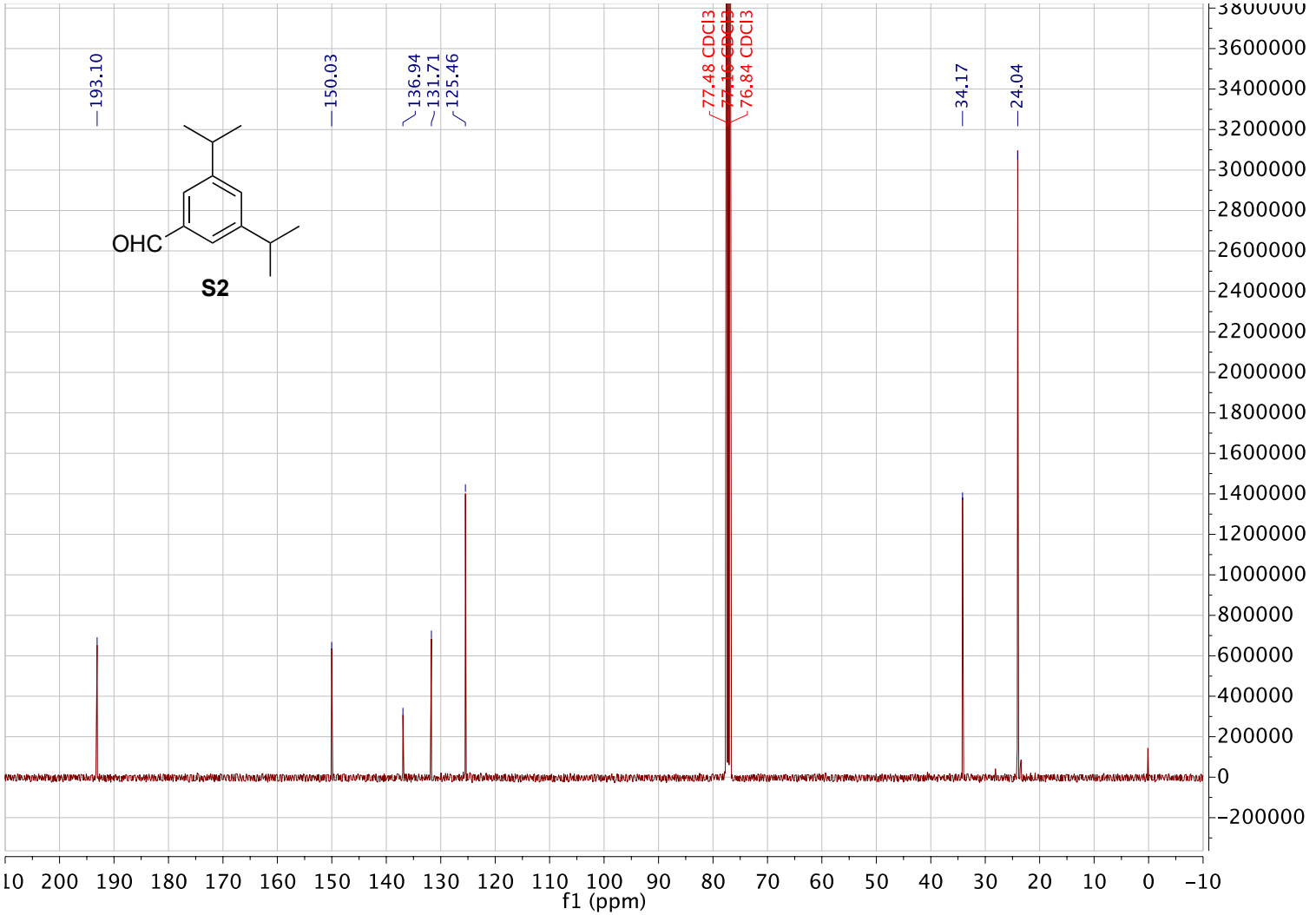

Mass Spectrum SmartFormula Report

Analysis Info

Analysis Name	D:\Data\User Data\Ode\000833_1-92_01_18965.d	Acquisition Date	2023/11/25 15:04:50
Method	lcms_esi_pos_low.m	Operator	BDAL@DE
Sample Name	000833	Instrument	micrOTOF II 8213750.10448
Comment			

Acquisition Parameter

Source Type	ESI	Ion Polarity	Positive	Set Nebulizer	3.0 Bar
Focus	Not active			Set Dry Heater	200 • ‹C
Scan Begin	50 m/z	Set Capillary	4500 V	Set Dry Gas	10.0 l/min
Scan End	2000 m/z	Set End Plate Offset	-500 V	Set Divert Valve	Waste

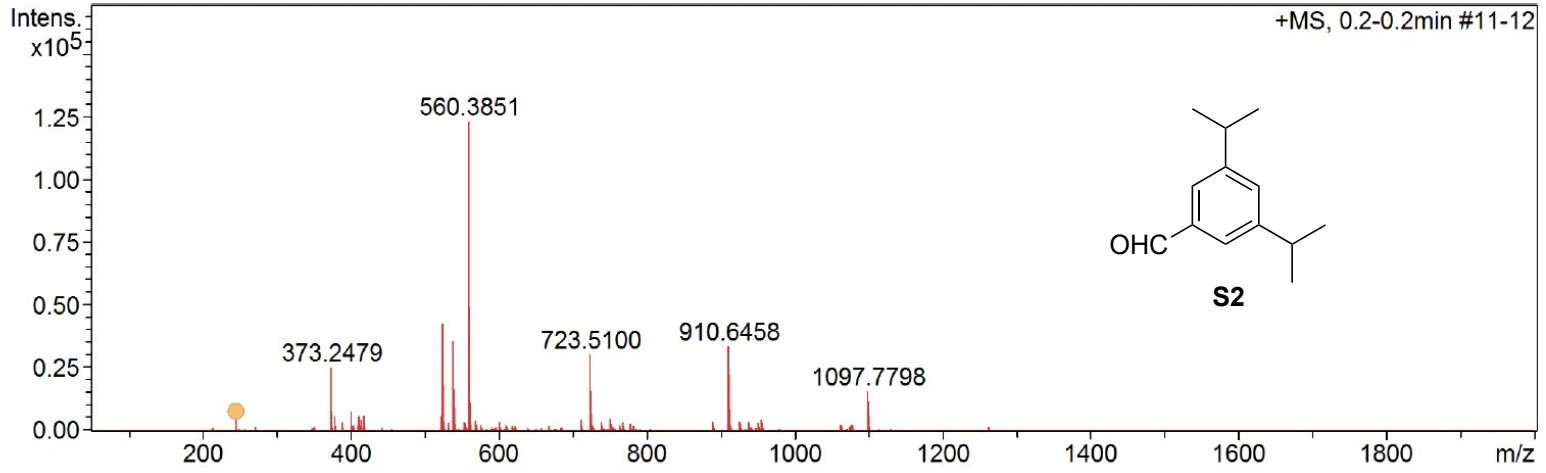

S2

Meas. m/z	#	Ion Formula	m/z	err [ppm]	mSigma	# mSigma	Score	rdb	e• P Conf	N-Rule
245.1509	1	C14H22NaO2	245.1512	1.1	3.2	1	100.00	3.5	even	ok

^{1}H-NMR in $CDCl_3$

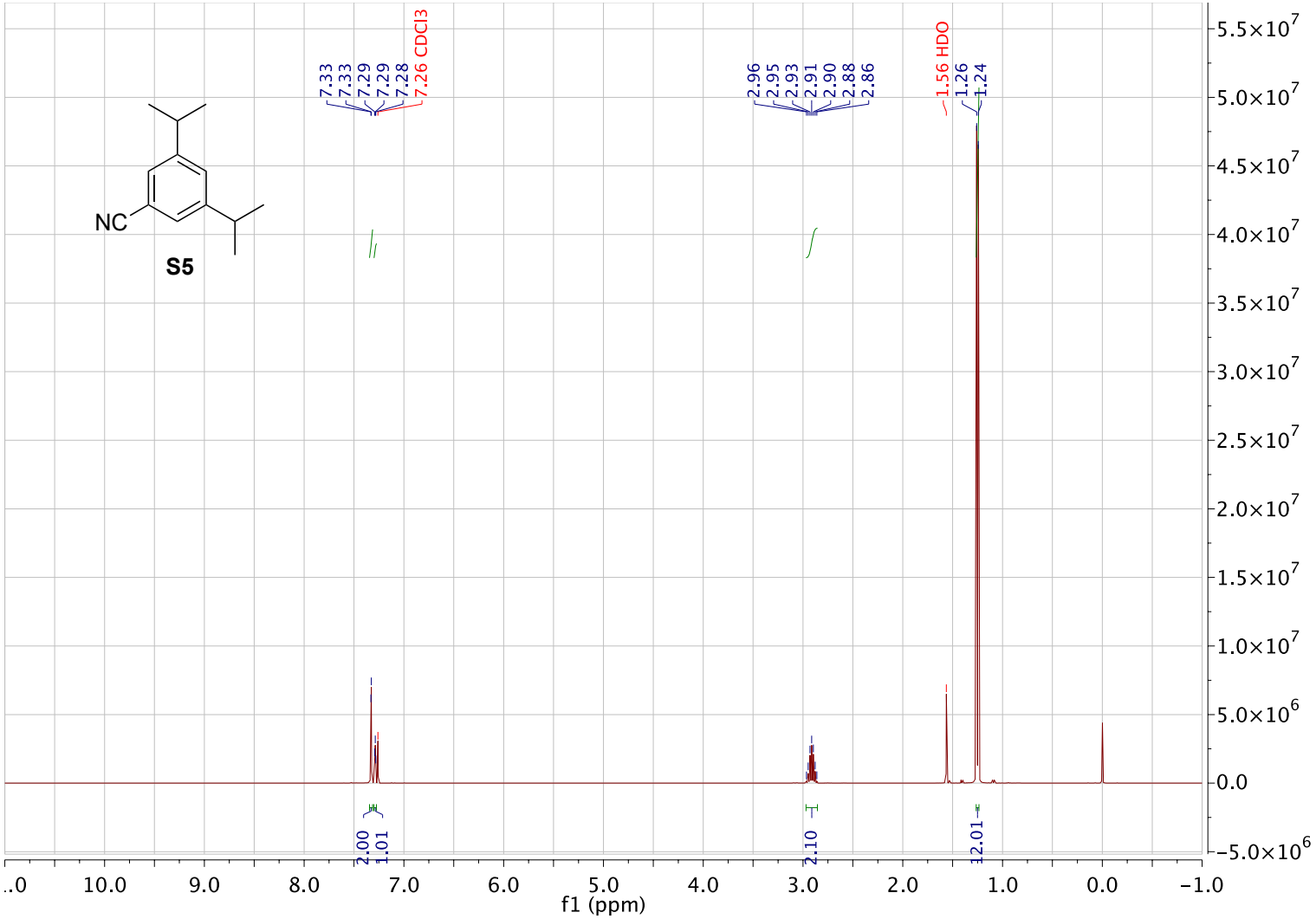

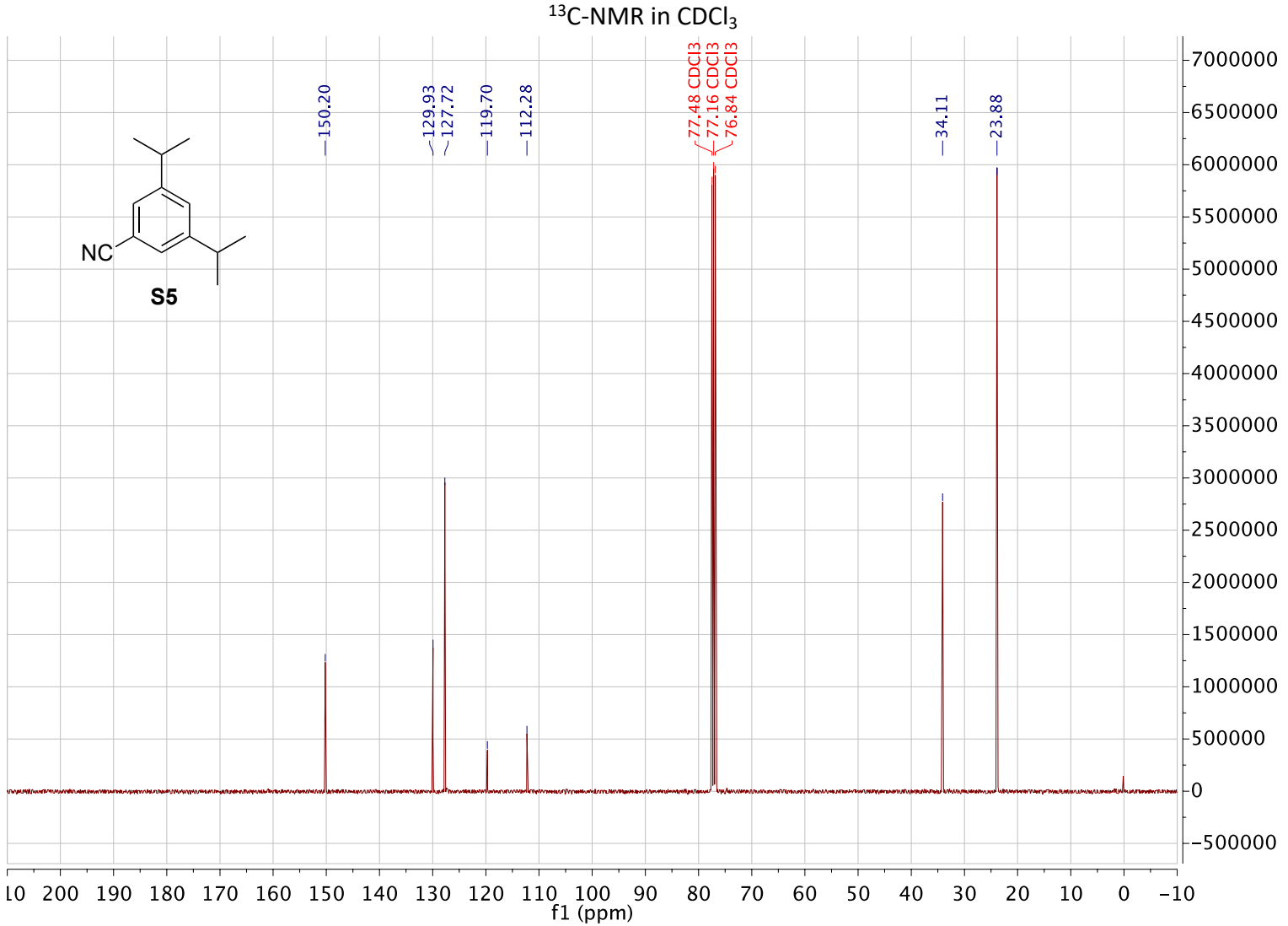
13C-NMR in CDCl3
NC
S5
150.20
129.93
127.72
119.70
112.28
77.48 CDCl3
77.16 CDCl3
76.84 CDCl3
34.11
23.88
f1 (ppm)

Mass Spectrum SmartFormula Report

Analysis Info

Analysis Name	D:\Data\User Data\Ode\000834_1-93_01_18966.d	Acquisition Date	2023/11/25 15:08:35
Method	lcms_esi_pos_low.m	Operator	BDAL@DE
Sample Name	000834	Instrument	micrOTOF II 8213750.10448
Comment			

Acquisition Parameter

Source Type	ESI	Ion Polarity	Positive	Set Nebulizer	3.0 Bar
Focus	Not active			Set Dry Heater	200 • ‹C
Scan Begin	50 m/z	Set Capillary	4500 V	Set Dry Gas	10.0 l/min
Scan End	2000 m/z	Set End Plate Offset	-500 V	Set Divert Valve	Waste

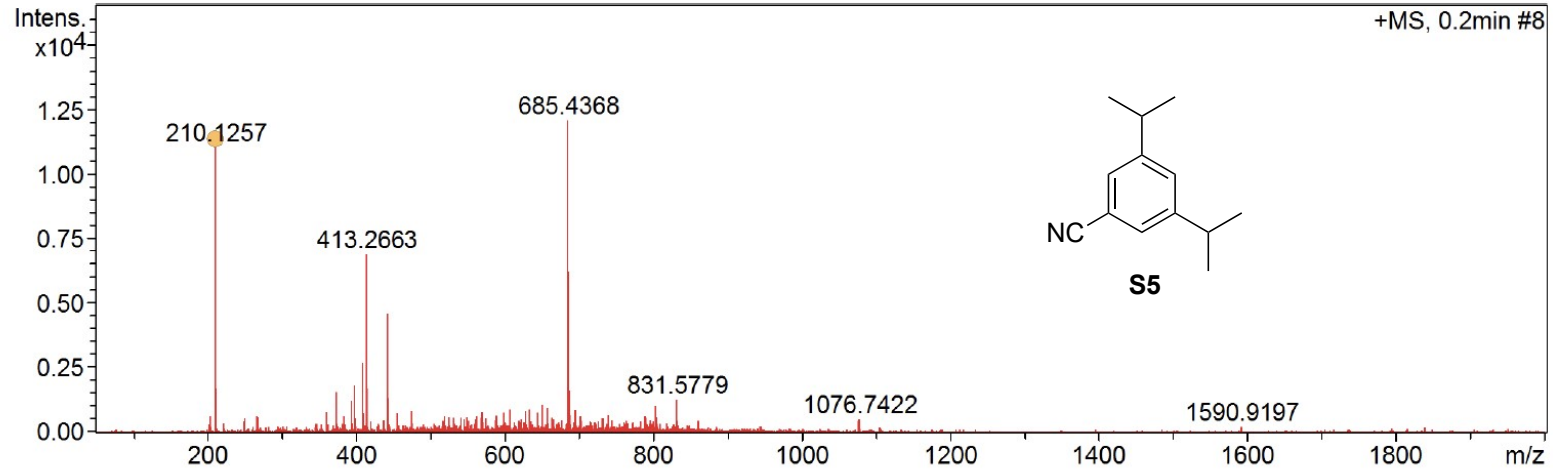

Meas. m/z	#	Ion Formula	m/z	err [ppm]	mSigma	# mSigma	Score	rdb	e• P Conf	N-Rule
210.1257	1	C13H17NNa	210.1253	-1.9	4.5	1	100.00	5.5	even	ok

^{1}H-NMR in $CDCl_3$

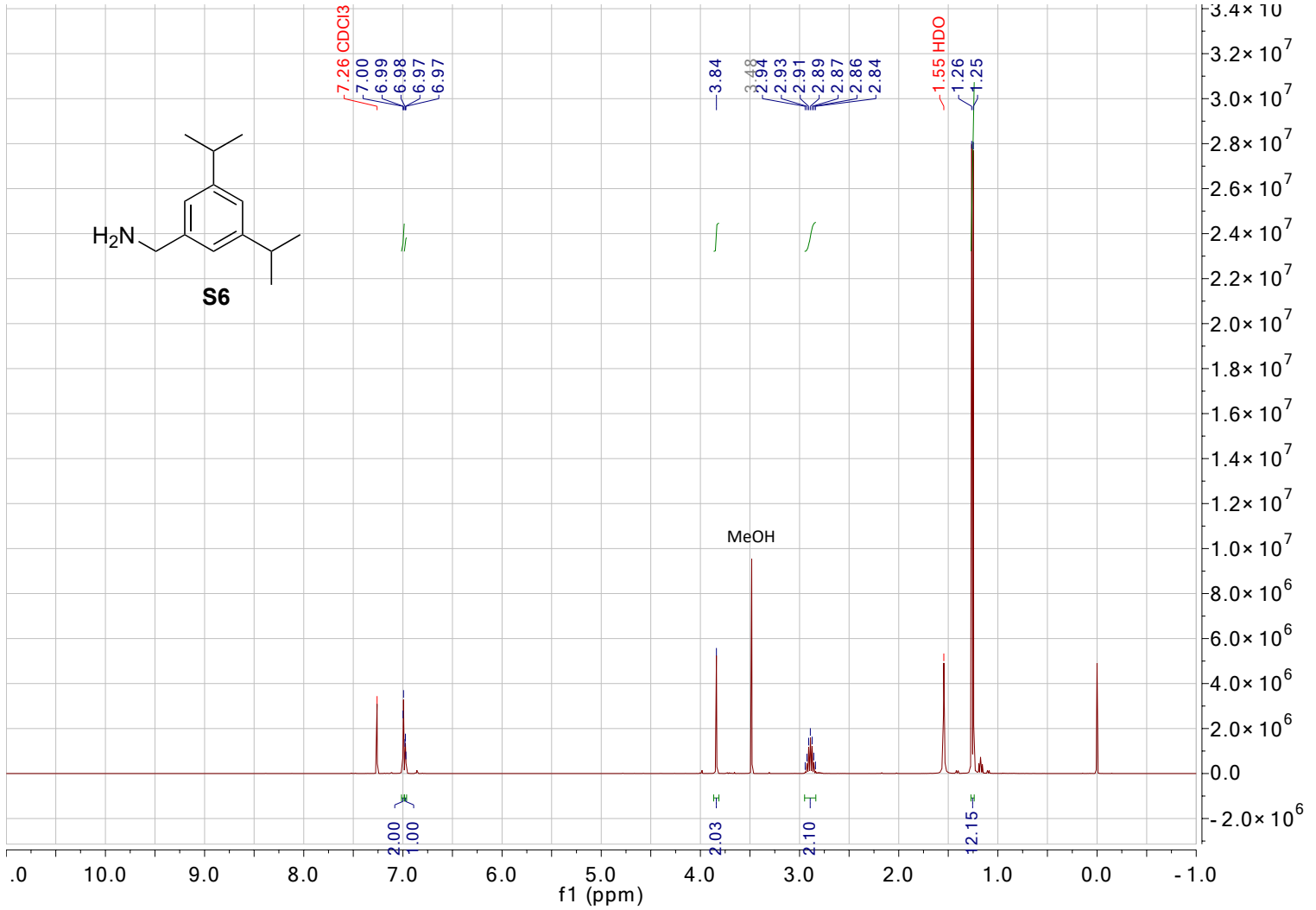

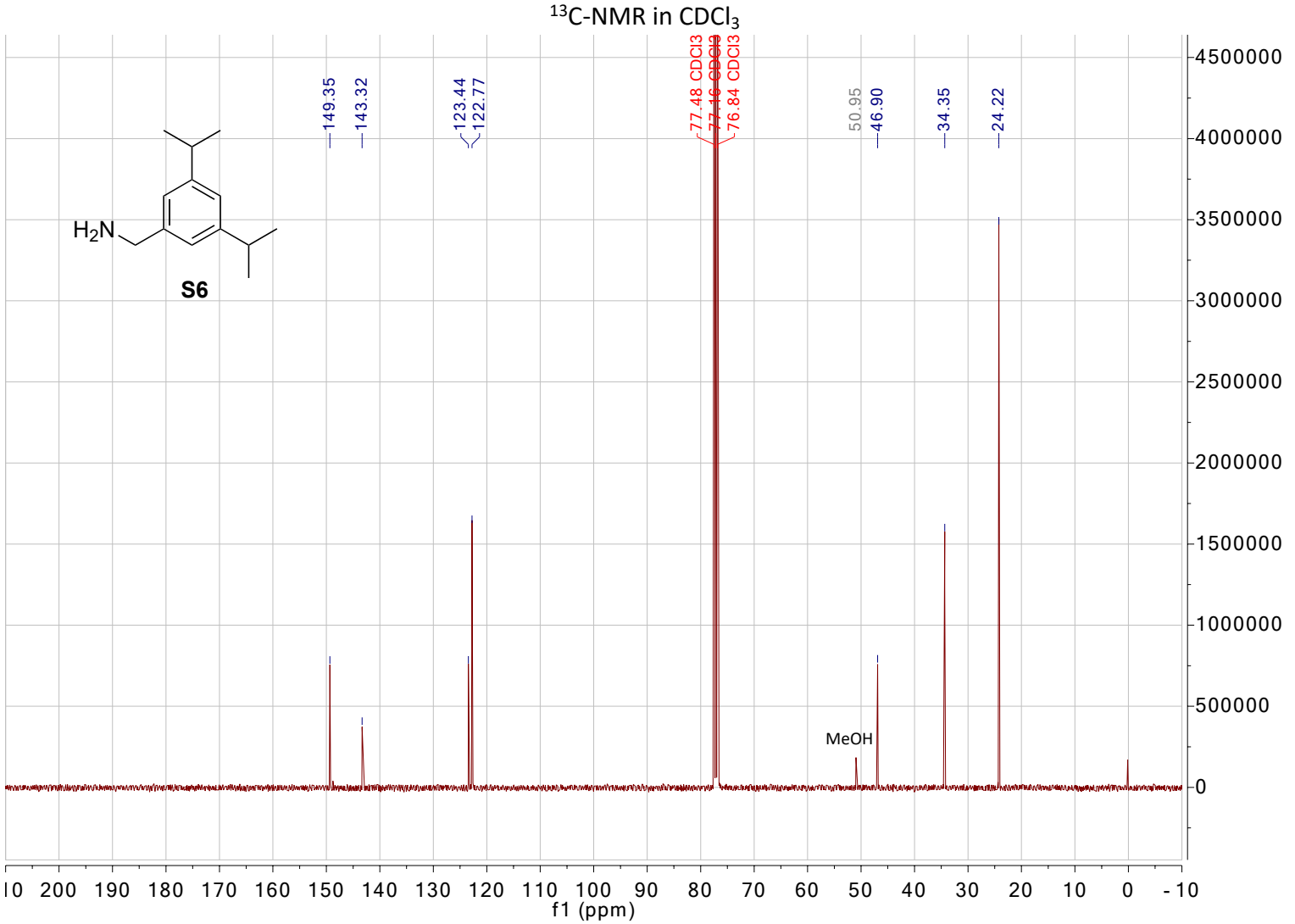
^{13}C-NMR in $CDCl_3$
H_2N
S6
149.35
143.32
123.44
122.77
77.48 CDCl3
77.16 CDCl3
76.84 CDCl3
50.95
46.90
34.35
24.22
MeOH
4500000
4000000
3500000
3000000
2500000
2000000
1500000
1000000
500000
0
f1 (ppm)

Mass Spectrum SmartFormula Report

Analysis Info

Analysis Name	D:\Data\User Data\Ode\000824_1-95_01_18228.d	Acquisition Date	2023/10/01 21:33:50
Method	lcms_esi_pos_low.m	Operator	BDAL@DE
Sample Name	000824	Instrument	micrOTOF II 8213750.10448
Comment			

Acquisition Parameter

Source Type	ESI	Ion Polarity	Positive	Set Nebulizer	3.0 Bar
Focus	Not active			Set Dry Heater	200 • ‹C
Scan Begin	50 m/z	Set Capillary	4500 V	Set Dry Gas	10.0 l/min
Scan End	2000 m/z	Set End Plate Offset	-500 V	Set Divert Valve	Waste

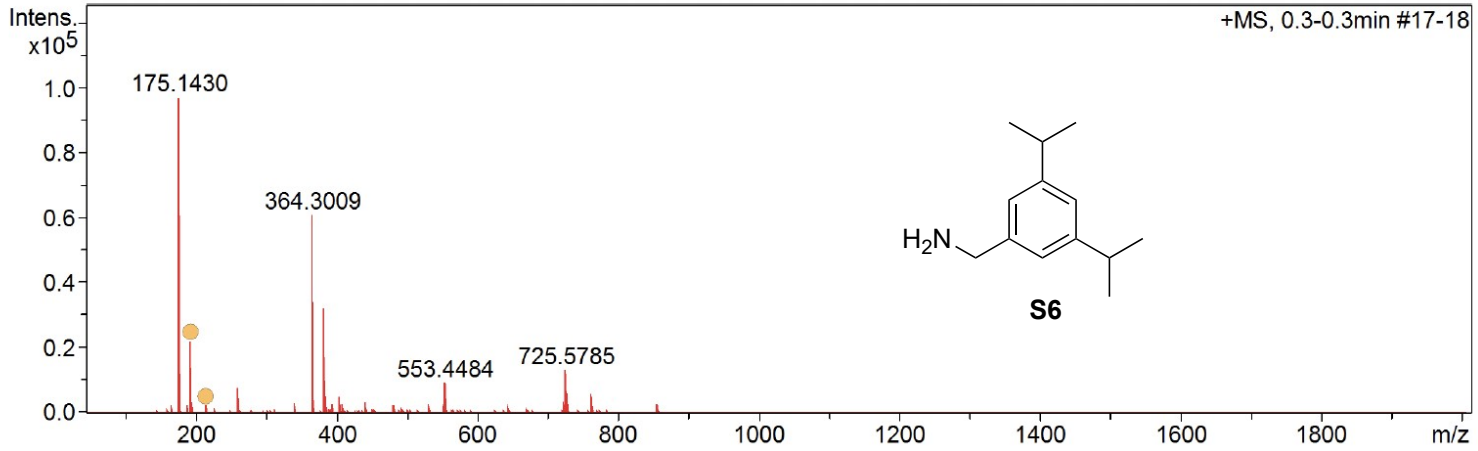

Meas. m/z	#	Ion Formula	m/z	err [ppm]	mSigma	# mSigma	Score	rdb	e• P Conf	N-Rule
192.1721	1	C13H22N	192.1747	13.7	5.8	1	100.00	3.5	even	ok
214.1566	1	C13H21NNa	214.1566	0.1	6.9	1	100.00	3.5	even	ok

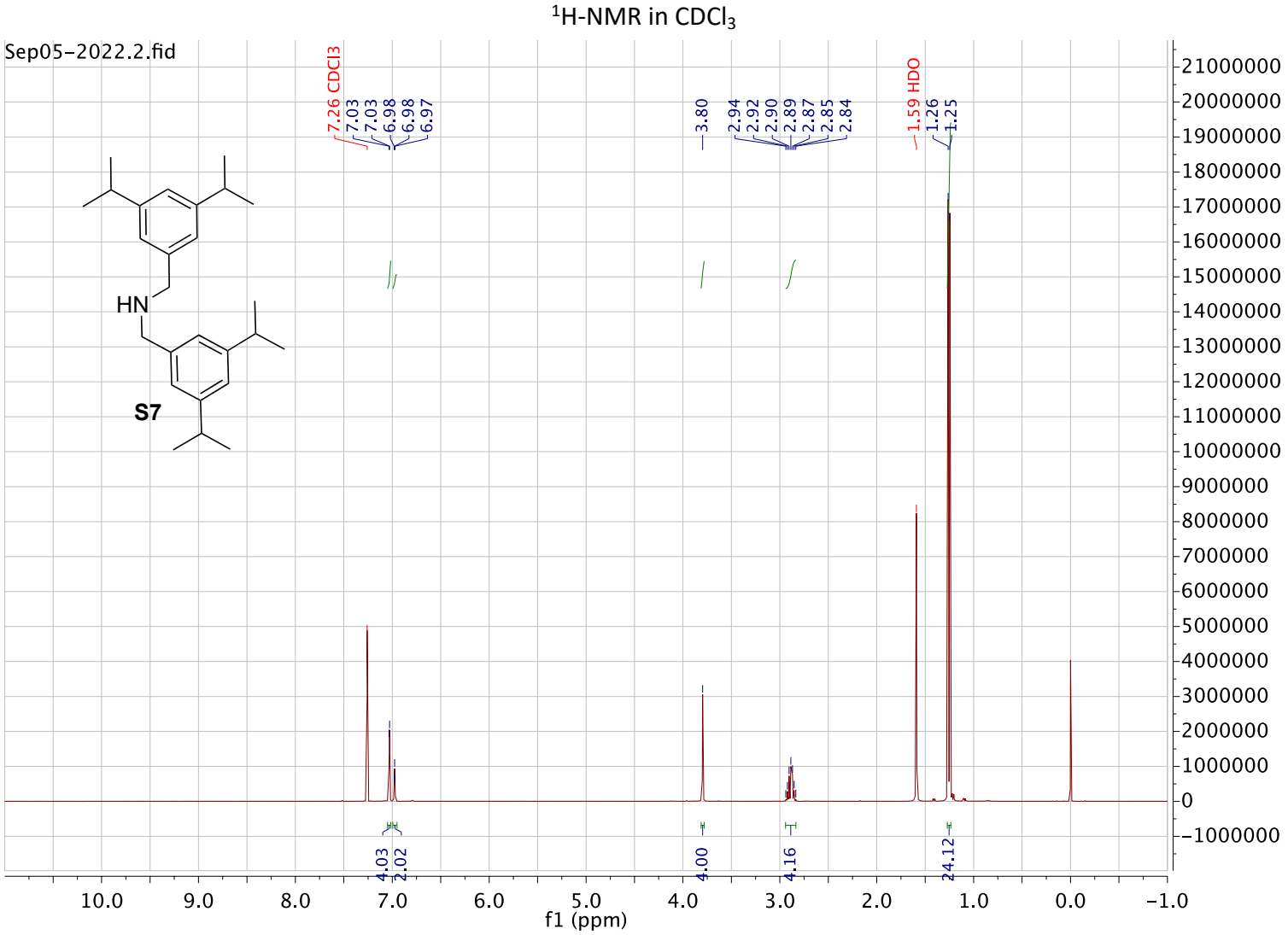
^{1}H-NMR in $CDCl_3$
Sep05-2022.2.fid
7.26 CDCl3
7.03
7.03
6.98
6.98
6.97
3.80
2.94
2.92
2.90
2.89
2.87
2.85
2.84
1.59 HDO
1.26
1.25
HN
S7
4.03
2.02
4.00
4.16
24.12
f1 (ppm)

^{13}C-NMR in $CDCl_3$

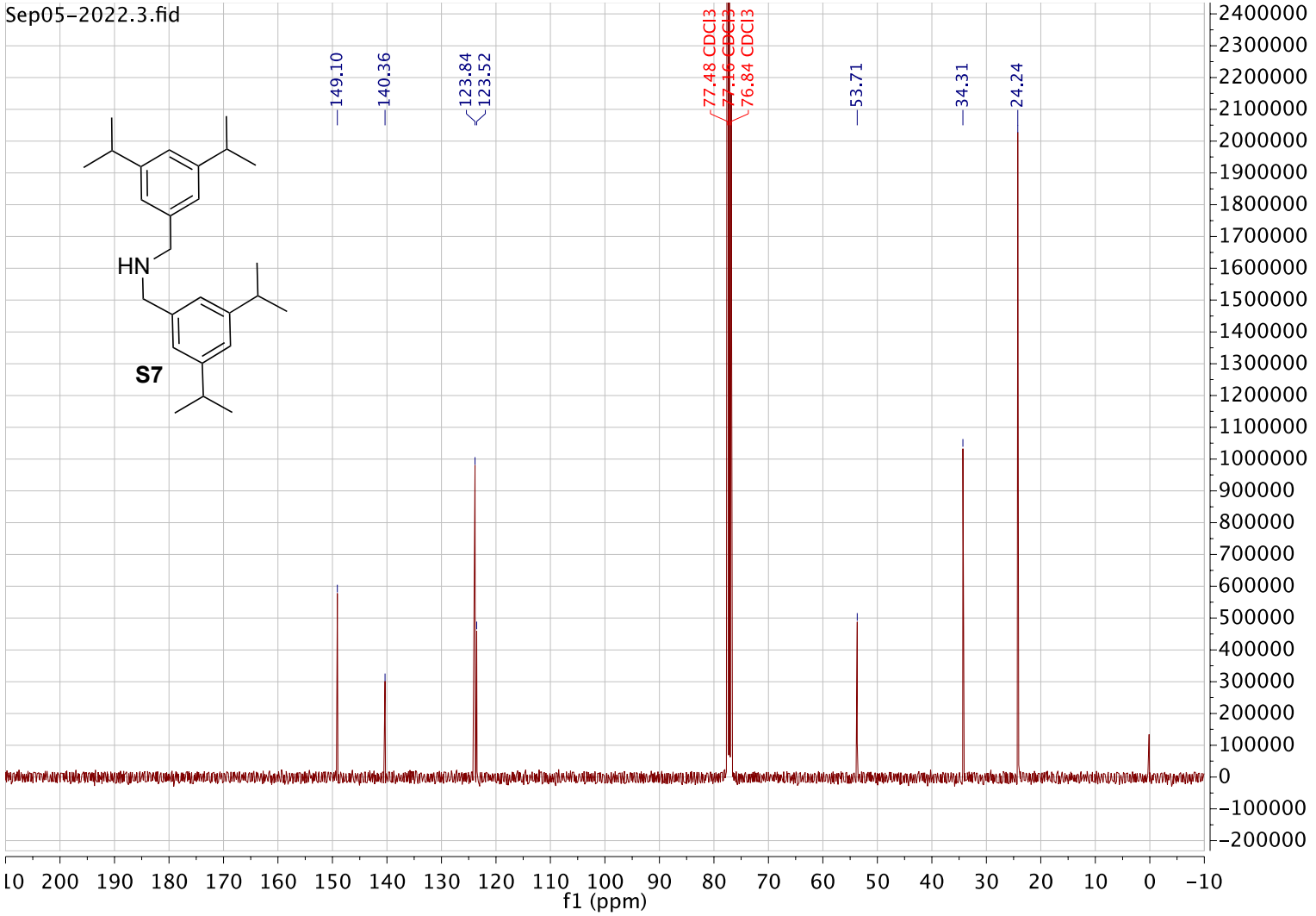

Mass Spectrum SmartFormula Report

Analysis Info

Analysis Name	D:\Data\User Data\Ode\000830_1-101_01_18234.d	Acquisition Date	2023/10/01 21:56:17
Method	lcms_esi_pos_low.m	Operator	BDAL@DE
Sample Name	000830	Instrument	micrOTOF II 8213750.10448
Comment			

Acquisition Parameter

Source Type	ESI	Ion Polarity	Positive	Set Nebulizer	3.0 Bar
Focus	Not active			Set Dry Heater	200 • ‹C
Scan Begin	50 m/z	Set Capillary	4500 V	Set Dry Gas	10.0 l/min
Scan End	2000 m/z	Set End Plate Offset	-500 V	Set Divert Valve	Waste

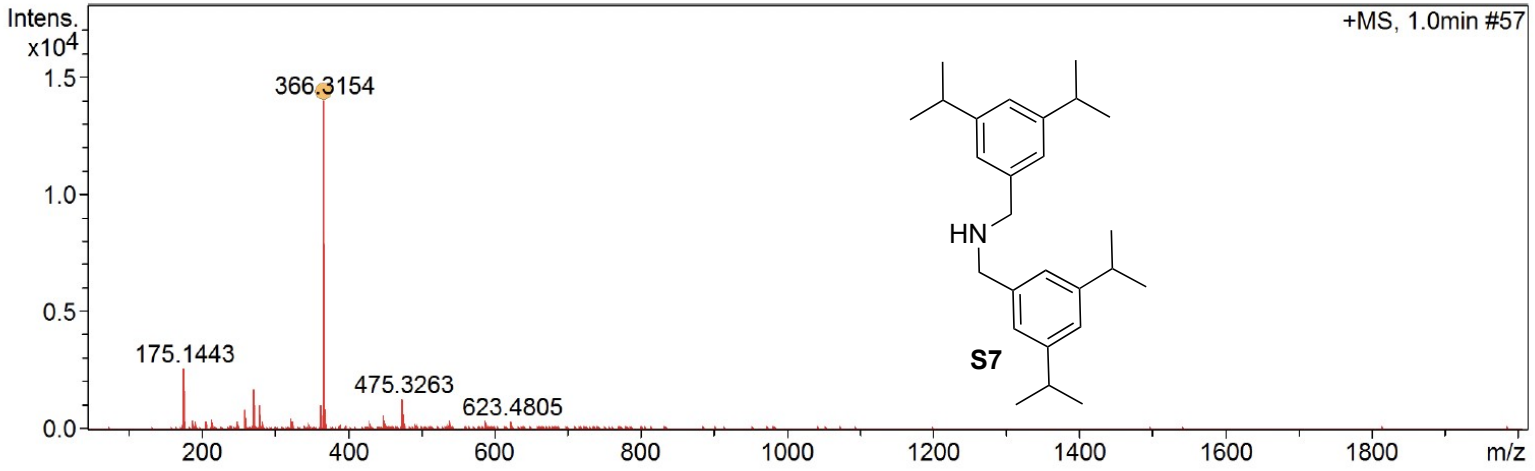

Meas. m/z	#	Ion Formula	m/z	err [ppm]	mSigma	# mSigma	Score	rdb	e• P Conf	N-Rule
366.3154	1	C26H40N	366.3155	0.2	21.8	1	100.00	7.5	even	ok

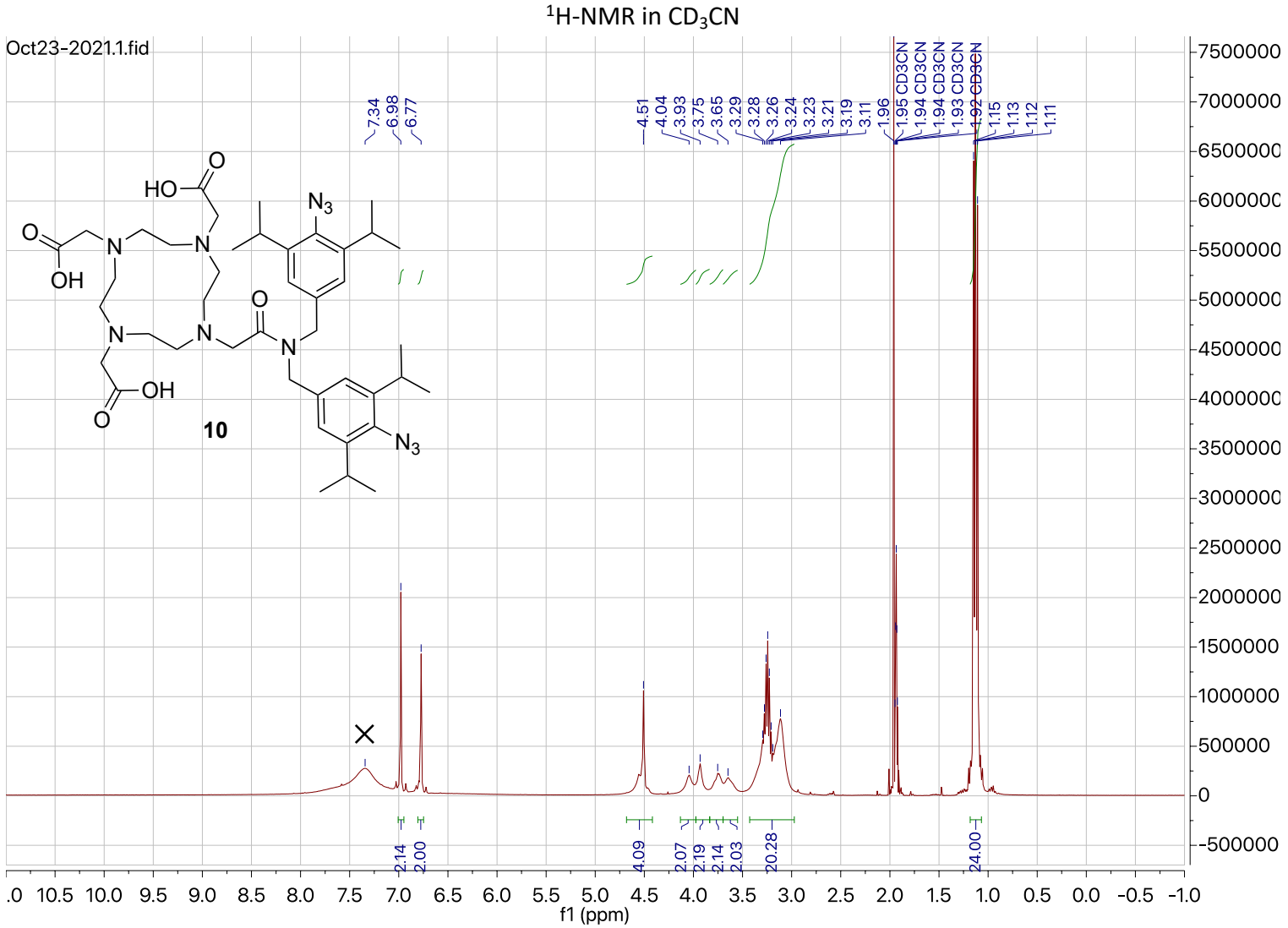
^{1}H-NMR in CD_3CN
Oct23-2021.1.fid
10
f1 (ppm)

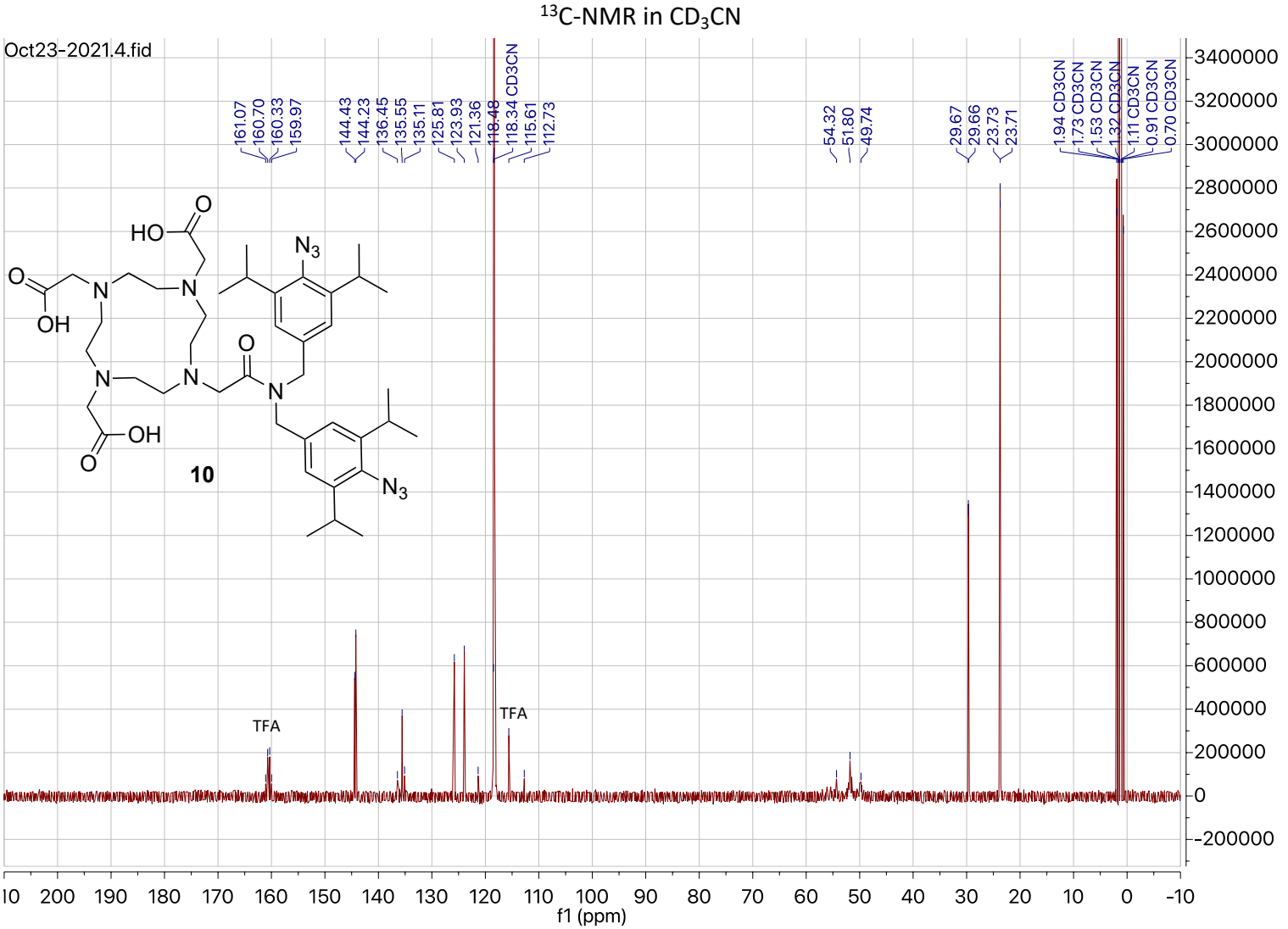
^{13}C-NMR in CD_3CN
Oct23-2021.4.fid
161.07
160.70
160.33
159.97
144.43
144.23
136.45
135.55
135.11
125.81
123.93
121.36
118.48
118.34 CD3CN
115.61
112.73
54.32
51.80
49.74
29.67
29.66
23.73
23.71
1.94 CD3CN
1.73 CD3CN
1.53 CD3CN
1.32 CD3CN
1.11 CD3CN
0.91 CD3CN
0.70 CD3CN
HO
O
O
OH
N
N
N
N
N
O
N
N_3
O
OH
O
N_3
10
TFA
TFA
f1 (ppm)

Mass Spectrum SmartFormula Report

Analysis Info

Analysis Name	D:\Data\User Data\Ode\000825_1-96_01_18229.d	Acquisition Date	2023/10/01 21:37:32
Method	lcms_esi_pos_low.m	Operator	BDAL@DE
Sample Name	000825	Instrument	micrOTOF II 8213750.10448
Comment			

Acquisition Parameter

Source Type	ESI	Ion Polarity	Positive	Set Nebulizer	3.0 Bar
Focus	Not active			Set Dry Heater	200 • ‹C
Scan Begin	50 m/z	Set Capillary	4500 V	Set Dry Gas	10.0 l/min
Scan End	2000 m/z	Set End Plate Offset	-500 V	Set Divert Valve	Waste

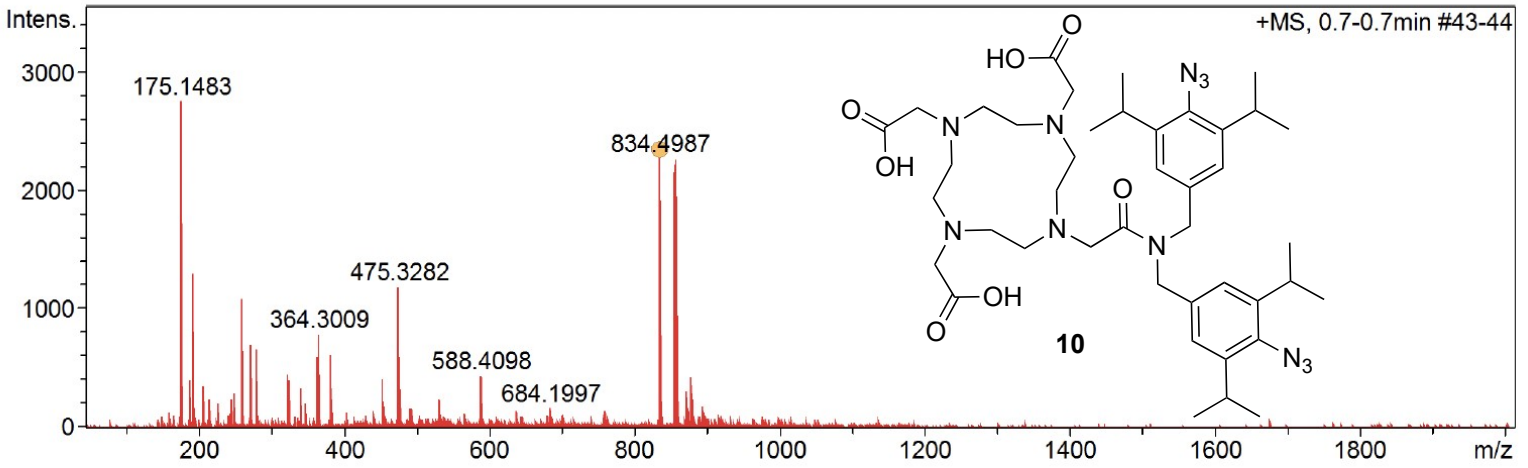

Meas. m/z	#	Ion Formula	m/z	err [ppm]	mSigma	# mSigma	Score	rdb	e• P Conf	N-Rule
834.4987	1	C42H64N11O7	834.4985	-0.3	17.2	4	100.00	16.5	even	ok

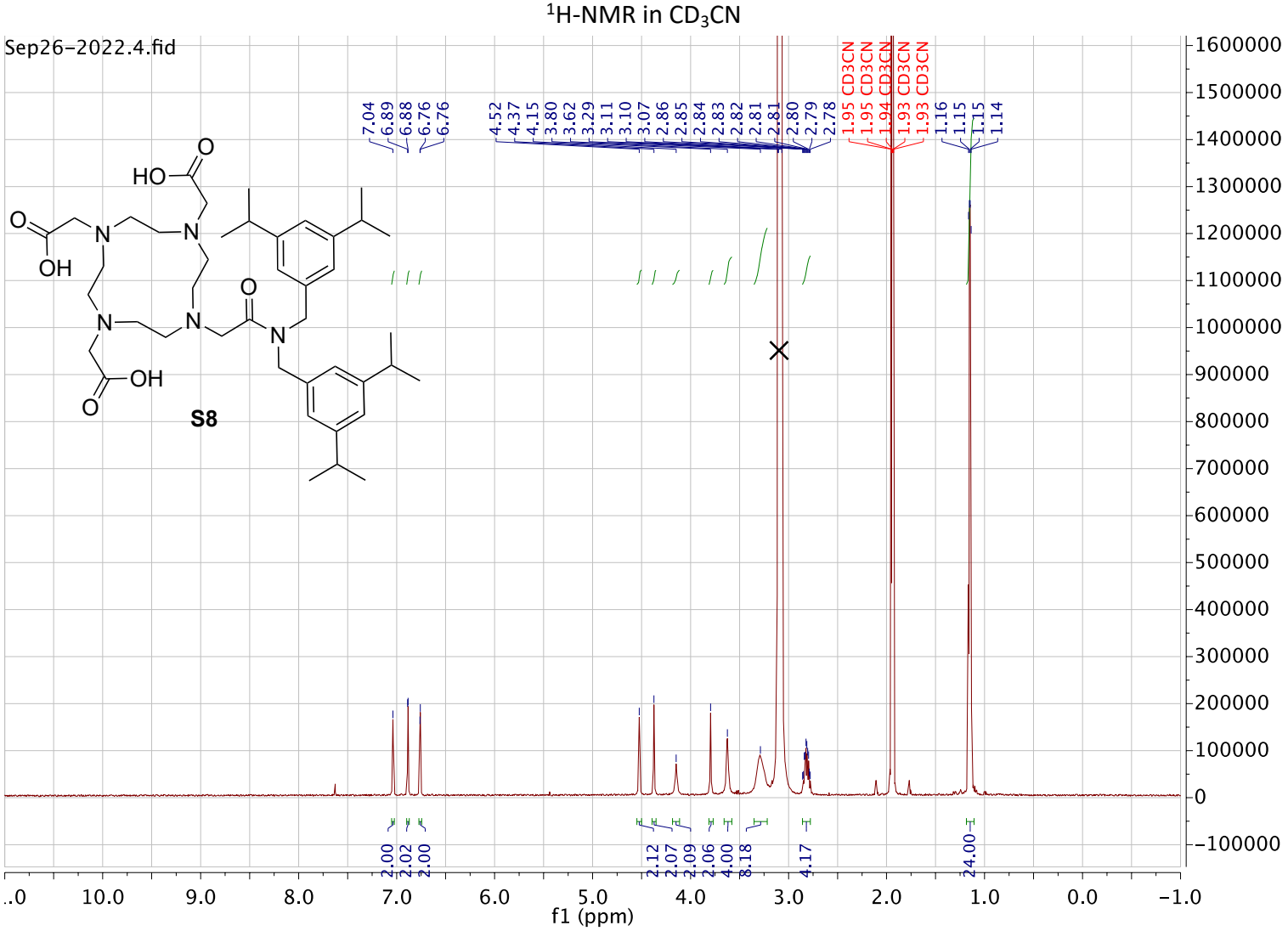
^{1}H-NMR in CD_3CN
Sep26-2022.4.fid
S8
f1 (ppm)

^{13}C-NMR in CD_3CN

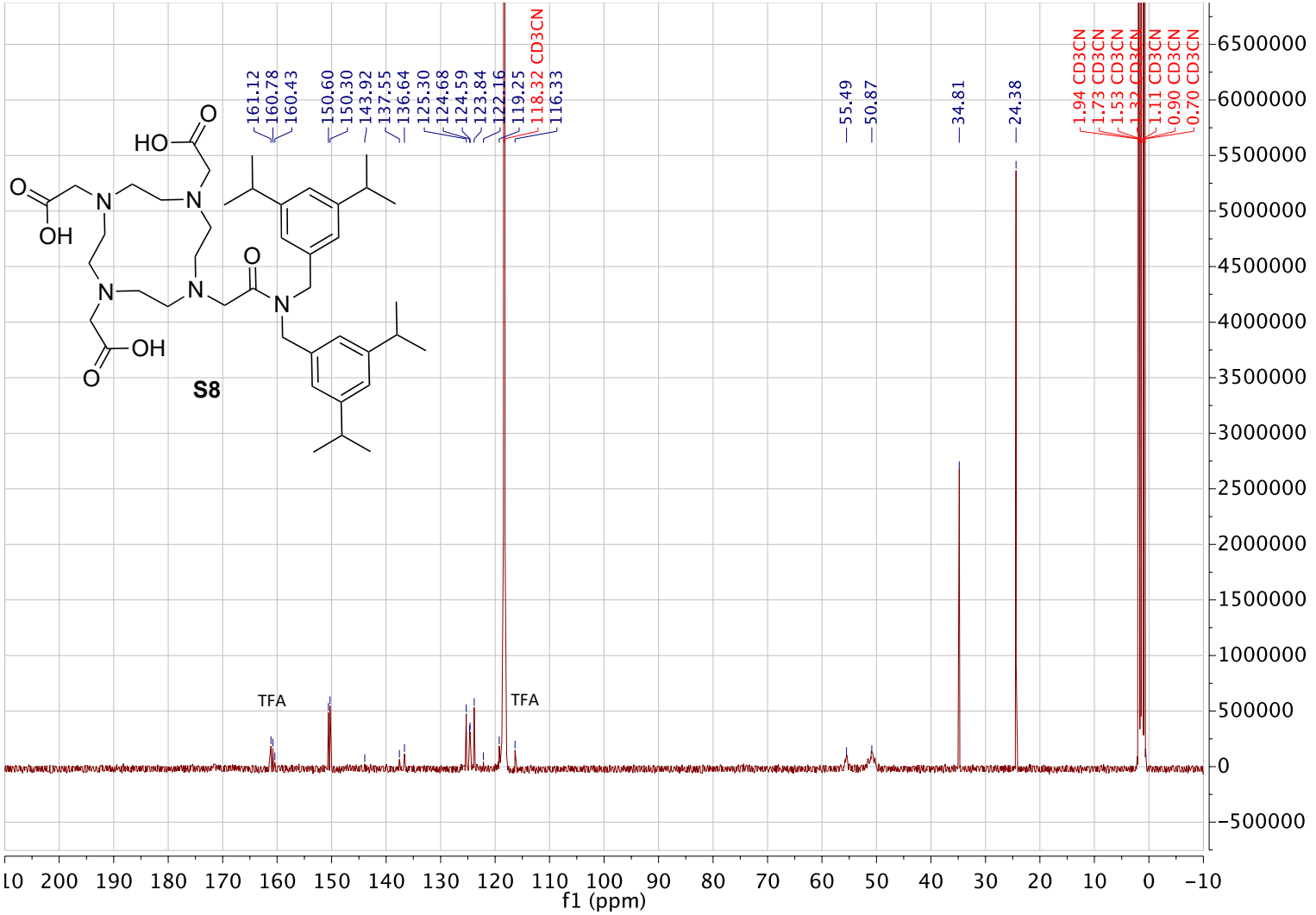

HRMS

Mass Spectrum SmartFormula Report

Analysis Info

Analysis Name	D:\Data\User Data\Ode\000826_1-97_01_18230.d	Acquisition Date	2023/10/01 21:41:16
Method	lcms_esi_pos_low.m	Operator	BDAL@DE
Sample Name	000826	Instrument	micrOTOF II 8213750.10448
Comment			

Acquisition Parameter

Source Type	ESI	Ion Polarity	Positive	Set Nebulizer	3.0 Bar
Focus	Not active			Set Dry Heater	200 • ‹C
Scan Begin	50 m/z	Set Capillary	4500 V	Set Dry Gas	10.0 l/min
Scan End	2000 m/z	Set End Plate Offset	-500 V	Set Divert Valve	Waste

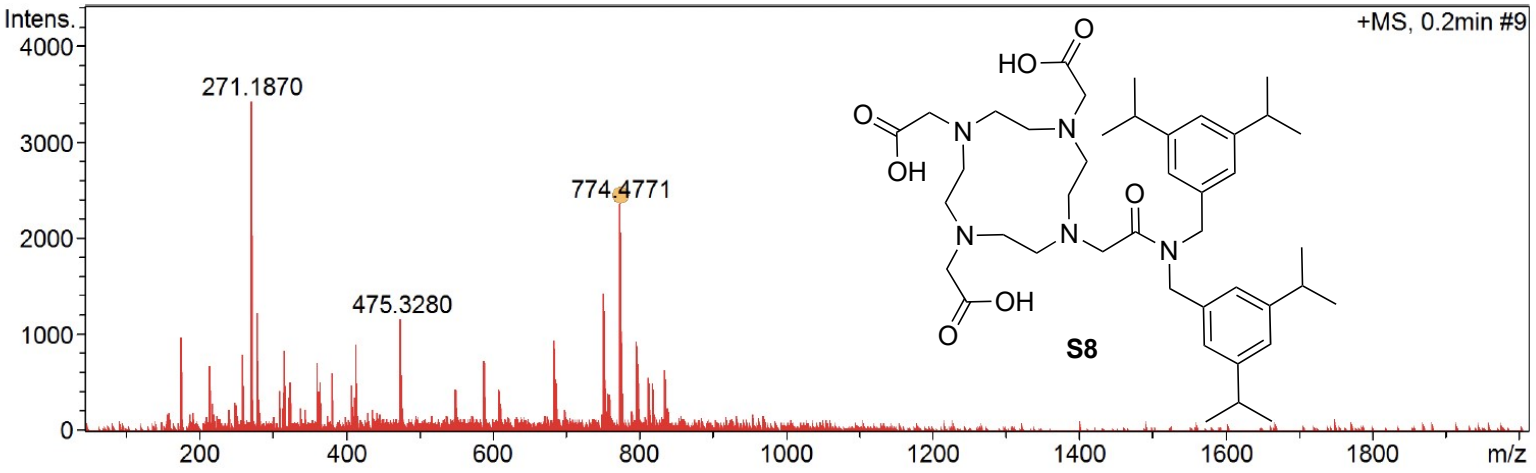

Meas. m/z	#	Ion Formula	m/z	err [ppm]	mSigma	# mSigma	Score	rdb	e• P Conf	N-Rule
774.4771	1	C42H65N5NaO7	774.4776	0.7	39.9	1	100.00	12.5	even	ok

^{1}H-NMR in CD_3CN

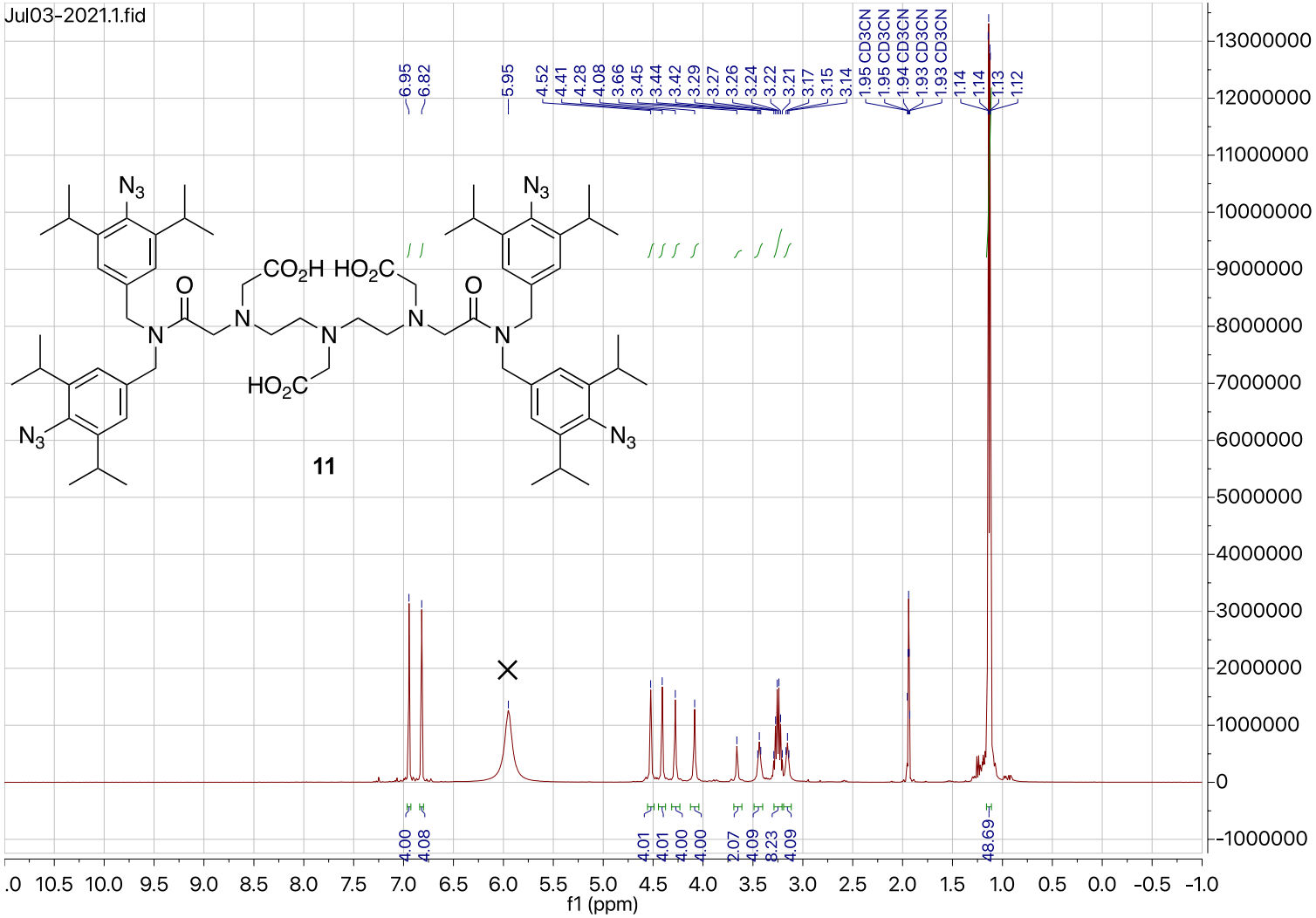

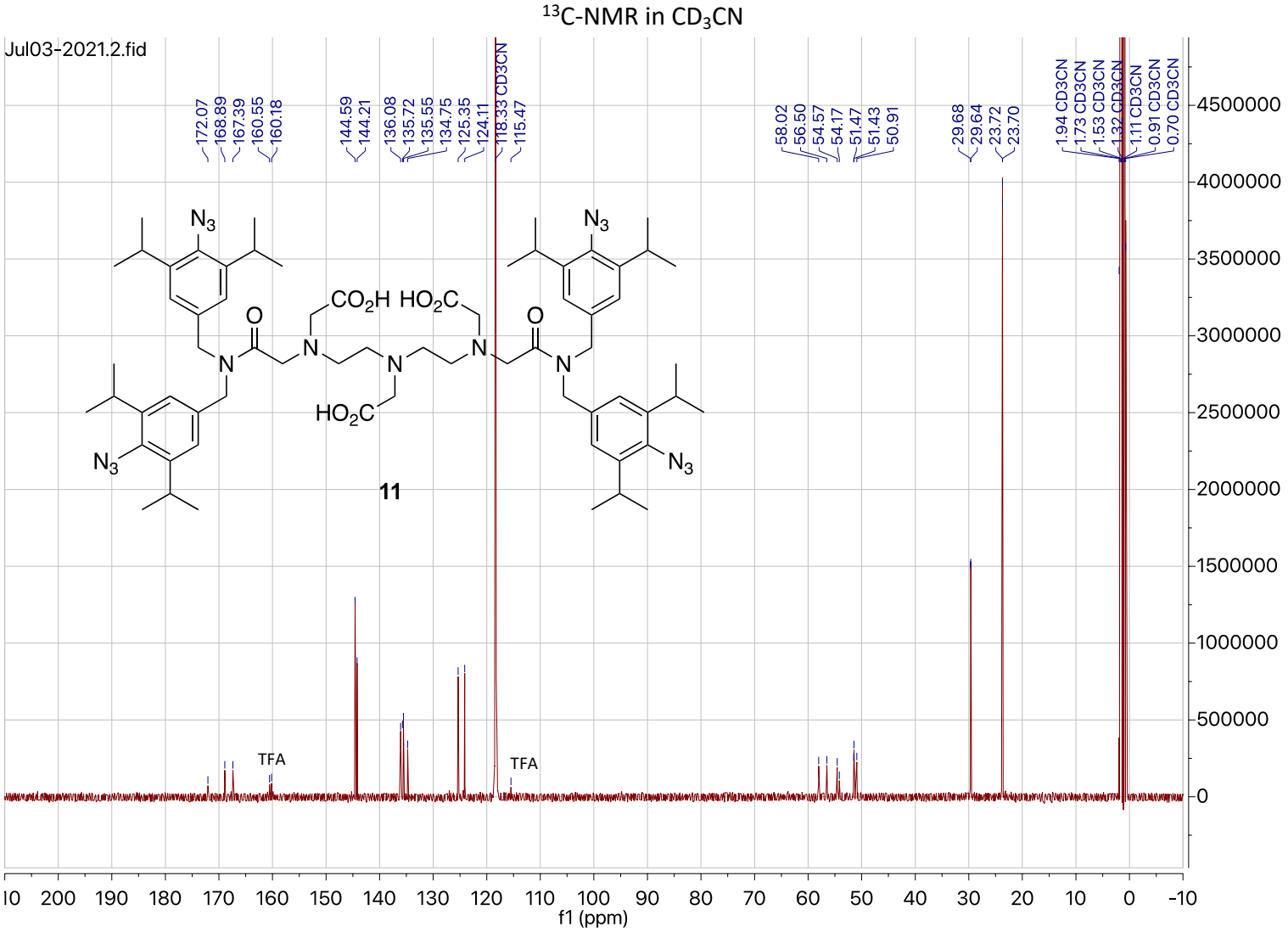
^{13}C-NMR in CD_3CN
Jul03-2021.2.fid
172.07
168.89
167.39
160.55
160.18
144.59
144.21
136.08
135.72
135.55
134.75
125.35
124.11
118.33 CD3CN
115.47
58.02
56.50
54.57
54.17
51.47
51.43
50.91
29.68
29.64
23.72
23.70
1.94 CD3CN
1.73 CD3CN
1.53 CD3CN
1.32 CD3CN
1.11 CD3CN
0.91 CD3CN
0.70 CD3CN
TFA
TFA
f1 (ppm)

11

Mass Spectrum SmartFormula Report

Analysis Info

Analysis Name	D:\Data\User Data\Ode\000827_1-98_01_18231.d	Acquisition Date	2023/10/01 21:44:59
Method	lcms_esi_pos_low.m	Operator	BDAL@DE
Sample Name	000827	Instrument	micrOTOF II 8213750.10448
Comment			

Acquisition Parameter

Source Type	ESI	Ion Polarity	Positive	Set Nebulizer	3.0 Bar
Focus	Not active			Set Dry Heater	200 • ‹C
Scan Begin	50 m/z	Set Capillary	4500 V	Set Dry Gas	10.0 l/min
Scan End	2000 m/z	Set End Plate Offset	-500 V	Set Divert Valve	Waste

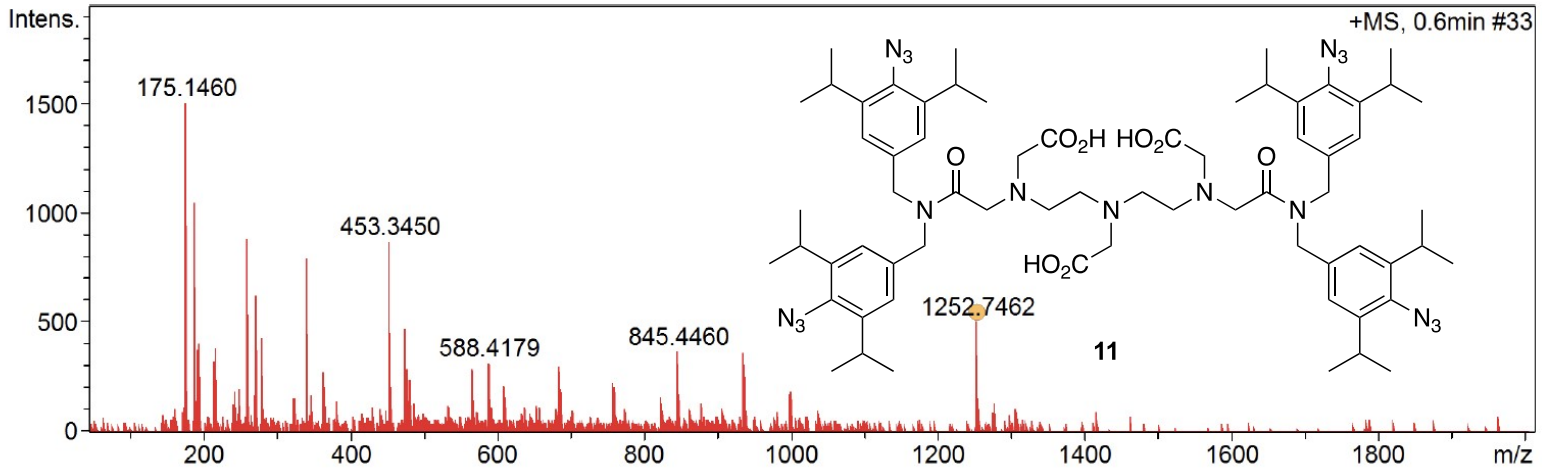

Meas. m/z	#	Ion Formula	m/z	err [ppm]	mSigma	# mSigma	Score	rdb	e• P Conf	N-Rule
1252.7462	1	C66H94N17O8	1252.7466	0.3	263.5	6	0.00	28.5	even	ok